CEDAR 2019

Eldorado Hotel
Santa Fe, New Mexico

MLT, Coupling, Instrumentation and Techniques
Poster Session
Tuesday June 18, 2019

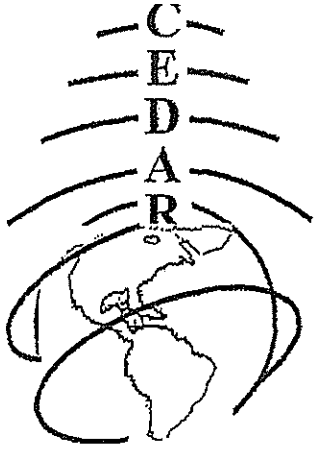

MLT Poster List

Coupling of the Upper Atmosphere with Lower Altitudes

Data Assimilation or Management

Instruments or Techniques for Middle Atmosphere Observations

MLTL Lidar Studies

Mesosphere or Lower Thermosphere General Studies

Solar Terrestrial Interactions in the Upper Atmosphere

Sprites

CEDAR Workshop – MLT, Coupling, Instrumentation and Techniques
Poster Session Abstracts
Day 1 – Tuesday, June 18, 2019

COUP01 - On the potential role of stratospheric ozone in atmosphere-ionosphere coupling during sudden stratosphere warmings - by Tarique Adnan Siddiqui

Status of First Author: Student NOT in poster competition PhD

Authors: Tarique Adnan Siddiqui, Astrid Maute, Nick Pedatella

Abstract: The last decade has seen major progress in the understanding of mechanisms responsible for upper atmosphere (mesosphere-lower thermosphere-ionosphere) variability during sudden stratospheric warming (SSW) events. The change of stratospheric circulation due to SSWs modulate the spectrum of vertically upward propagating atmospheric waves (gravity waves, tides, and planetary waves) resulting in numerous changes in the state of the upper atmosphere. Recent studies have confirmed that much of the upper atmospheric variability associated with SSWs is driven by changes in the migrating and nonmigrating solar tides. During SSWs, the planetary wave forcing induces a global circulation that leads to the buildup of ozone density and an enhancement in the longitudinal asymmetry of the ozone distribution in the tropics at stratospheric altitudes. These changes in the stratospheric ozone have the potential to affect the excitation mechanism of migrating and nonmigrating solar tides. This work aims to investigate the impact of ozone changes on the solar tides during SSWs for a better understanding of the mechanisms connecting the terrestrial and space weather. For this purpose, case study of the 2009 SSW event is carried out using the Whole Atmosphere Community Climate Model (WACCM) with two distinct simulation setups. In the first simulation, the ozone concentrations are interactively calculated in the model and resemble the observational ozone concentrations during the 2009 SSW event while in the second simulation, the ozone concentrations are climatologically specified. The variability of ozone during the 2009 SSW event is captured in the first simulation unlike the second one in which the ozone is prescribed. Thereafter, the migrating and nonmigrating solar tidal amplitudes are calculated from the model temperature and wind outputs in the mesosphere-lower thermosphere (MLT) region for both these simulations. The difference in the tidal amplitudes from these two model runs provides an estimate of the change that occurred in them due to the variability of ozone during the 2009 SSW event.

COUP02 - E Region Scintillation Variations Observed by FORMOSAT-3/COSMIC and Their Relation to Wind Shear Derived from GAIA - by Tzu-Ya Tai

Status of First Author: Student IN poster competition Masters

Authors: Tzu-Ya Tai, Loren C. Chang, Huixin Liu

Abstract: Gravity waves, planetary waves and atmospheric tides from the lower atmosphere propagating upwards may cause ionospheric perturbations resulting in scintillation. Recent studies have shown that these coupling effects can be manifested in E region scintillation. By using the S4 index from FORMOSAT-3/COSMIC radio occultation observations from 2009 to 2012 and Ground-to-topside model of Atmosphere and Ionosphere for Aeronomy (GAIA), we investigate the regional morphology of the vertical ion convergence that leads to the formation of sporadic E layers, equatorial plasma bubble (EPB) and their relation with wind shear in the mesosphere and lower thermosphere region. The S4 index occurrence position observed by FORMOSAT-3/COSMIC radio occultation from 2009 to 2012 in East Asia were compared with the distribution of vertical ion convergence derived from GAIA, in order to

determine the relation to the actual scintillation occurrence. Based on the result, we will discuss the predictability of scintillation occurrences by using FORMOSAT-3/COSMIC and GAIA.

COUP03 - Tidal Forcing Effects on the Zonal Variation of Solstice Equatorial Plasma Bubbles - by Loren Chang

Status of First Author: Non-student PhD

Authors: Loren C. Chang, Cornelius Csar Jude H. Salinas, Yi-Chung Chiu, Pei-Yun Chiu, McArthur Jones Jr., Charles C.H. Lin

Abstract: Equatorial plasma bubbles are elongated plasma depletions that can occur in the nighttime ionospheric F region, causing scintillation in satellite navigation and communications signals, and manifesting in ionograms as spread F. Equatorial plasma bubbles are believed to be Rayleigh-Taylor instabilities seeded by vertically propagating gravity waves. A necessary pre-condition for plasma bubble formation is believed to be a threshold vertical ion drift from the E region, which is required to produce the vertical plasma gradients conducive to such an instability. Factors affecting the zonal and seasonal variation of equatorial plasma bubbles therefore include magnetic declination, as well as the strength of the equatorial electojet, and neutral winds in the lower thermosphere controlling vertical plasma drifts via the wind dynamo. In most longitude zones, the above factors result in elevated occurrence rates of equatorial plasma bubbles during the equinoxes. The notable exception is over the central Pacific and African sectors, where equatorial plasma bubble activity maximizes during solstice. As the zonal separation of the two sectors is roughly half the Earth's circumference, Tsunoda et al. (2015) hypothesized that the solstice maxima in these two sectors could be driven by a zonal wavenumber 2 atmospheric tidal component in the mesosphere and lower thermosphere (MLT). In this study, we find that the post-sunset electron density observed by FORMOSAT-3/COSMIC during the boreal summer does indeed exhibit a wave-2 zonal distribution in both the equatorial and northern mid latitude regions. The equatorial wave-2 is consistent with results expected from elevated vertical ion drift over the Central Pacific and African sectors, while the mid- latitude wave-2 is consistent with the Mid-Summer Nighttime Anomaly. Using COSMIC, the seasonal, longitudinal, and local time variation of ionospheric tidal and stationary planetary wave (SPW) components that produce zonal wavenumber 2 disturbances when viewed in a constant local time frame is examined. Numerical experiments are also carried out using the Thermosphere Ionosphere lectrodynamics General Circulation Model (TIE-GCM) to determine the effect of the aforementioned tidal and SPW components on vertical ion drift, showing a clear wave-2 modulation of vertical ion drift when subject to forcing from wave-2 atmospheric tidal components in the mesosphere and lower thermosphere. The aforementioned results are consistent with the solstice maxima hypothesis.

COUP04 - Atmosphere and ionosphere responses to infrasonic acoustic waves driven by the 2016 Kaikoura earthquake - by Pavel Inchin

Status of First Author: Student IN poster competition Masters

Authors: P.A. Inchin, J.B. Snively, Y. Kaneko, M.D. Zettergren

Abstract: One of the largest recent earthquakes in New Zealand – Kaikoura Mw 7.8 in 2016, attracted a lot of attention from scientific community due to the unusual complexity of multi-segmented faulting process [Hamling et al., Sci., 2017]. Even today, some aspects of the rupture dynamics are not fully understood. The dense network of Global Navigational Satellite Systems (GNSS) stations in New Zealand allowed investigations of the ionospheric response to this event, revealing some of its distinctive features. In particular, Bagiya et al. [JGR, 2018] studied the characteristics of coseismic ionospheric disturbances

(CIDs) and demonstrated that they are linked to two separate surface rupture zones. Based on a newly developed back-projection technique and kinematic rupture modeling with point sources, Lee et al. [BSSA, 2018] also confirmed that the initial rupture did not cause significant energy to be radiated into the atmosphere. Instead, the near-coastal uplift resulted in the generation of the strongest acoustics in atmosphere. Li et al. [2018, JGR] speculated that features of CIDs found ~20 min after the rupture initiation can also be explained by the complexity of faulting processes. Here we model the atmospheric and ionospheric responses of the Kaikoura earthquake based on realistic time- and spatial-dependent surface displacements driven by this earthquake. The kinematic slip model of Holden et al. [2017] that fits local strong-motion accelerometer and high-rate GPS data is used to model the surface displacements. This kinematic source model captures a complex pattern of rupturing process from the south to north, including rupture reactivation on the Kekerengu fault 60 seconds after the origin time. The simulated surface vertical displacement field is then used as a bottom boundary condition for 3D neutral atmosphere model MAGIC, which is in turn coupled with 2D ionosphere model GEMINI [Zettergren and Snively, JGR, 2015] to simulate generation, propagation and dissipation of acoustic and gravity waves and driving of CIDs. Modeling reveals the primary features of infrasonic waves signatures driven by near-field displacements, providing important basis for the understanding of coupling processes. Being a nighttime event, we also investigate the possible utility of ionospheric TEC and airglow measurements together for these studies.

COUP05 - Inter-hemispheric coupling during SSW events observed using WACCM-X model - by Kashyapa Narenathreyas

Status of First Author: Student NOT in poster competition PhD

Authors: Kashyapa Narenathreyas, Amal Chandran

Abstract: In this study, we present results from Whole Atmosphere Community Climate Model (WACCM-X) illustrating the inter-hemispheric coupling phenomenon during Stratospheric Sudden Warming (SSW) events. In particular, we focus on those years which experience an elevated stratopause after a discontinuity of the stratopause due to the SSW. In this study, we characterize the response of the summer mesosphere to: 1) the heating period, and 2) the elevated stratopause period and find differences in the response of the summer mesosphere to changing conditions in the opposite hemisphere stratosphere. We show composites made from multiple free-running WACCM-X simulations of the period 2000-2014 and show that the temperature anomalies and changes in residual circulation and zonal mean winds observed are statistically significant. WACCM-X simulations often show a mesospheric cooling in the summer hemisphere at the time of the SSW (averaged over 5 days of the central date of an SSW) while the summer mesosphere shows a warming during the extended recovery period and elevated stratopause period following an SSW. We analyse the anomalies and momentum fluxes in order to deduce and propose a mechanism behind those coupled dynamics. We validate these results with observations the Microwave Limb Sounder Instruments on the Aura satellite.

COUP06 - Volcano-generated Ionospheric Disturbances: Comparison of GITM-R simulations with GNSS observations - by Justin Tyska

Status of First Author: Student IN poster competition Undergraduate (checked)

Authors: Cissi Y. Lin, Yue Deng

Abstract: Disturbances through propagation of the developed acoustic gravity waves (AGWs). These disturbances can be observed by ground based and spaceborne Global Navigation Satellite Systems (GNSS) and used to analyze various properties of the initial perturbation such as localization, direction, and total energy content. The focus of this study is to simulate ionospheric Total Electron Content (TEC) variations induced by volcanic eruption using a GCM and to subsequently compare the simulations with the GNSS data. Unlike tsunamis and earthquakes, volcanic eruption is more or less like a point source at a fixed geographic location causing relatively localized perturbation. Simulations using Global Ionosphere-Thermosphere Model with local refinement (GITM-R) are performed to capture subtleties in the regions near the volcano as well as its effects on a larger scale as variations have been known to propagate as wide as ~800 km. GITM's lower boundary is at ~100 km altitude and thus a variety of possible forcing functions are imposed at the localized lower boundary and resulting ionospheric TEC variations are compared to observational data in an attempt to classify which one most accurately reproduces the volcanic disturbances and the dependence of TEC variations on the features of AGWs imposed at the lower boundary.

COUP07 - Modeling ionospheric responses to earthquakes in the near field - by Xing Meng

Status of First Author: Non-student PhD

Authors: Attila Komjathy, Olga P. Verkhoglyadova, Giorgio Savastano, Mattia Crespi, Michela Ravanelli

Abstract: Vertical ground movement during earthquakes could excite upward-propagating acoustic-gravity waves in the atmosphere resulting in electron density perturbations in the ionosphere. Such ionospheric perturbations have been detected by a number of ionospheric observational techniques, including the Global Navigation Satellite System (GNSS) measurements used to derive ionospheric total electron content (TEC). To understand the observed ionospheric perturbations and study the earthquake-ionosphere coupling processes, we have developed an analytical Wave Perturbation (WP) model coupled to the state-of-the-art Global Ionosphere-Thermosphere Model (GITM). The coupled model, WP-GITM, is capable of simulating the thermospheric and ionospheric perturbations induced by the epicentral movement during earthquakes. Model validations against GNSS-derived TEC observations have shown promising results. However, this previous version of WP-GITM assumes a point source representing the epicentral crustal movement, which neglects the radiation pattern of a seismic source. Moreover, it does not solve the ionospheric perturbations induced by Rayleigh surface waves propagating away from the epicenter. In this work, we aim to replace the point source with an extended area source and include the Rayleigh-surface waves, so that the earthquake-induced ionospheric perturbations in the near-field region (within about 1000km from the epicenter) can be better modeled. The updated WP-GITM is driven by seismic ground motion measurements from two or more locations surrounding an epicenter. The ground motion data is obtained with GPS measurements using the Variometric Approach for Displacements Analysis Stand-alone Engine (VADASE). We apply the model to simulate the ionospheric response to the 16 September 2015 Illapel, Chile earthquake, validate the simulated TEC perturbations against GNSS observations, and compare the modeling results to those obtained from the previous point-source model.

COUP08 - Using Physics-based Simulations to Study the Influences of Day-to-Night Flow in the Thermosphere - by Zachary Waldron

Status of First Author: Student IN poster competition PhD

Authors: Zachary Waldron, Jeffrey Thayer, Eric Sutton

Abstract: The magnitude of differences between the daytime and nighttime thermosphere neutral mass density is an indicator of the day-to-night general circulation and controlling factors thereof. Muller et al. (2009) studied these differences in the context of the neutral density day-to-night ratio as measured by the CHAMP satellite. In this study, we extend their work by including physics-based simulations to diagnose the various influences of the day-to-night flow. Using ephemeris data from the CHAMP satellite to sample the model at all positions and times along the CHAMP orbit from 2002 to 2005, we then calculate the day-to-night ratio of mass density using the same analysis procedures as Muller et al. (2009). This study serves to validate the model's accuracy relative to the CHAMP data, and to determine the model's sensitivity to various factors, such as external drivers, lower boundary conditions, and viscous and ion drag forcing. Using this method, we also aim to move towards identifying and isolating diurnal variations from the errors caused by external forcing in the context of a recently developed data assimilation technique.

COUP09 - Study of Medium-Scale Traveling Ionospheric Disturbances Observed in the South American Equatorial and Low Latitude Region - by Patrick Essien

Status of First Author: Student IN poster competition PhD

Authors: Essien P., Takahashi, H., Figueiredo, C. A. O. B, Wrasse, C. M, Barros, D. , Gobbi, D., Lomotey, S. O.

Abstract: Total electron content (TEC) fluctuation in the ionosphere is one of the main unresolved problems on navigation systems, related to degrading resolution and reliability of the ground positioning. The South American low/equatorial latitude ionospheric region is where the highest spatial and temporal variations of TEC and various features of the ionosphere such as Medium-Scale Traveling Ionospheric Disturbances (MSTIDs) among others can be found. Therefore, the need to study the MSTIDs that propagate in the regions is the main focus of the present work. Using data collected by GNSS (GLONASS and GPS specifically) dual frequency receivers network over the South American region, we developed detrending TEC maps to recognize the presence and characterize MSTIDs in terms of horizontal wavelength, period, phase velocity and propagation direction. Preliminary results obtained from the data in 2014 and 2015 are presented and discussed. We noted that atmospheric gravity waves could be one of the prime precursors of the MSTIDs observed.

COUP10 - Influences of migrating semidiurnal tide variabilities on the low latitude ionosphere - by Jia-Ting Lin

Status of First Author: Student IN poster competition PhD

Authors: J. T. Lin, C. H. Lin, L. C. Chang, H.-L. Liu and N. M. Pedatella

Abstract: In this study, we investigate the variability of ionosphere and its electrodynamic responses to various semi-diurnal migrating tide (SW2) variations associated with SSW using numerical experiments under solar minimum condition. The earlier phase shift of SW2 causes the morning-enhanced and afternoon-reduced TECs by modulating equatorial vertical ExB drift, which agrees with the observation qualitatively but with insufficient magnitude. The SW2 amplification, which previously considered as the main driver of ionosphere-SSW coupling, produces temporally ExB enhancement due to the westward acceleration of F-region zonal winds by SW2. Results from the experiment adopting both the phase shifted and amplified SW2 agree with the observation in both magnitude and long sustained ExB enhancement. Our results demonstrate that both phase shift and amplification of SW2 are required to reproduce ionospheric SSW effects.

COUP11 - Study of Medium-Scale Traveling Ionospheric Disturbances Using an Automatic Algorithm - by Ping-Hsuan Cheng

Status of First Author: Student IN poster competition Masters

Authors: P. H. Cheng, C.H. Lin

Abstract: This paper studies the Medium-Scale Traveling Ionospheric Disturbances (MSTID) and plasma bubbles statistically at the low-latitude equatorial ionization anomaly (EIA) region of ionosphere using the network of ~100GPS receivers in Taiwan during 2013-2015. The dynamic of MSTID is complex since there are several disturbance sources from the lower atmosphere could affect the growth of MSTID. To statistically study the MSTID and plasma bubble features, an autonomous MSTID and plasma bubble detection algorithm is developed for detection and distinction of their occurrences and direction of propagation by using both the three-dimensional fast Fourier transform (3D-FFT) and the machine learning. Trough the statistical study, we indicate the following characteristics. First, the southward MSTIDs were observed almost every evening and morning during spring and winter. On the contrary, southward MSTIDs were more discernible at midnight in summer but least observed in autumn. Second, northward MSTIDs were detected most frequently from noon to midnight in summer. Last but not least, sort of equatorial plasma bubbles occurrence rates in descending order is spring equinox, fall equinox, summer solstice, and winter solstice.

COUP12 - Infrasonic waves and multiple cusps in ionograms - by Justin Mabie

Status of First Author: Student NOT in poster competition PhD

Authors: Justin Mabie, Terrence Bullett

Abstract: Infrasonic waves generated after large earthquakes (M8.0 or greater) have long been known to cause structure in ionograms in the form of migrating or multiple cusps. Following a controlled experiment to observe a rocket induced infrasonic wave, multiple cusps are observed in ionograms. For the first time high temporal resolution observations are made of infrasonic wave induced plasma displacements at the same time that multiple cusps are observed in ionograms. These observations allow for a physical explanation of how and why multiple cusps form after large earthquakes.

COUP13 - Simulation of tropical cyclone induced concentric gravity wave propagation in the upper atmosphere - by Yuxin Zhao

Status of First Author: Student IN poster competition Masters

Authors: Yuxin Zhao; Yue Deng

Abstract: The tropical cyclone (TC) induced concentric gravity waves (CGWs) are capable of propagating upward from convective sources in the troposphere to the ionosphere and creating concentric traveling ionosphere disturbances (CTIDs). To examine the CGWs propagation, we implement tropical cyclone induced CGWs into the global ionosphere–thermosphere model (GITM), which is a three-dimensional (3-D) non-hydrostatic general circulation model for the upper atmosphere. In this study, we simulate the CGWs induced by super typhoon "Meranti" in 2016. The shape and move trails of the wave are obtained from tropical cyclone best track dataset and the wave patterns are obtained from time evolution of the band-pass filtered total electron contents (TECs). The simulation results reveal a clear scenario of ionospheric CTIDs and neutral density and electron density perturbations in upper atmosphere.

DATA01 - Scheduling and Analysis Software for the LAICE Cubesat - by Cameron Earle

Status of First Author: Student IN poster competition Undergraduate

Authors: Cameron Earle, Stephen Noel, Namrata Kedia

Abstract: The Lower Atmosphere/Ionosphere Coupling Experiment (LAICE) is a 6U Cubesat developed by Virginia Tech (VT) and the University of Illinois (UIUC). The mission is slated to be manifested for deployment from the ISS in 2020. It carries VT instrumentation to measure ion and neutral gravity wave-induced density variations in low Earth orbit, and UIUC photometers to image waves in the mesosphere. We have developed a suite of two applications to manage the scheduling and data analysis aspects of the mission, as well as potential future missions. The command scheduling and generation portion of the software is a web-based application that runs in any browser in the science operations center at VT. It comprises a simple interface to schedule commands that allow the user to choose instrument state, modes, and duty cycles. The application is implemented in two parts: a backend written in Kotlin (Java derivative)

using the Spring Boot web application development framework; and a frontend implemented as a Single-Page Application (SPA) in JavaScript. The data analysis portion of the software is a desktop application written in Kotlin to provide versatile visualization of the science data collected by the satellite. The application can be configured to display data from any combination of onboard VT instruments. Additionally, it can display individual IV curves from the onboard RPA to allow the data quality to be assessed. Combining the two applications creates a versatile, user friendly interface to facilitate command uplinking and data analysis tasks.

DATA02 - Prediction of geomagnetically-induced currents: performance limitations, thresholds, and initial results using a machine-learning approach - by Matthew Grawe

Status of First Author: Student NOT in poster competition Masters

Authors: Matthew Grawe, Jonathan Makela, Farzad Kamalabadi

Abstract: Prediction of geomagnetically-induced currents (GICs) during space weather events is of critical importance to the safety and security of large-scale power distribution systems. Developing a quantitative understanding of the performance limitations and requirements inherent to these predictions (whether they are achieved using empirical or first-principles approaches) carries significant value and informs those responsible for the future deployment of supporting instrumentation. Here, we quantitatively discuss these performance limitations in the specific case of L1-to-ground GIC prediction, develop performance thresholds for three semi-recent space weather events, and provide some initial empirical prediction results using various machine learning approaches.

DATA03 - Preliminary result of a comprehensive analysis of low-latitude variability of ionsopheric electrodynamics using data assimilation - by Chih-Ting Hsu

Status of First Author: Non-student PhD

Authors: Chih-Ting Hsu, Tomoko Matsuo, Astrid Maute, Russel Stoneback, Chuan-Ping Lien

Abstract: The goal of this study is to conduct a quantitative data-driven and first-principles-based investigation to improve the understanding of the variability of ionospheric electrodynamics. The dominant sources of ionospheric variability originate from the Sun and the lower atmosphere. These external drivers are highly changeable, and it is often difficult to measure them continuously and globally. Therefore, estimating the uncertainty and variability of energy sources and evaluating their impact on the ionosphere are crucial steps for a better understanding of the physical mechanisms behind observed ionospheric variability. Data assimilation can help quantify the effects of these energy sources by combining multiple types of observations with guidance from first-principles models. To generate the variability of the ionosphere due to uncertainty and variability of energy from the lower atmosphere, the MERRA-driven TIME-GCM will be incorporated into TIE-GCM as a lower boundary condition. The AMIE and solar irradiance data will be used to generate the variability of the ionosphere caused by the uncertainty and variability of the energy from magnetosphere and the Sun. Meanwhile, both COSMIC electron density and C/NOFS ion velocity data are going to be assimilated into the TIE-GCM in order to provide a comprehensive vision of the dayside, low-latitude, and global-scale variability of ionospheric electrodynamics.

DATA04 - A deep Learning Based Approach to Predict the Onset of Magnetic Substorms - by Maimaitirebike Maimaiti

Status of First Author: Student IN poster competition PhD

Authors: M. Maimaiti, B. Kunduri, J. M. Ruohoniemi, J. B. H. Baker

Abstract: The magnetic substorm has been extensively studied over the past five decades using observations from instruments like magnetometers as well as through first principles based models and yet our understanding of its driving mechanisms is limited and so is our ability to accurately forecast its onset. In this study, we present the first deep learning based approach to predict the onset of a magnetic substorm, as defined by the SuperMAG SML index. Specifically, we use a time history of solar wind and interplanetary magnetic field (IMF) parameters as inputs to forecast the occurrence probability of onset over the next 1 hour. The model is trained on the SuperMAG list of ~36000 geomagnetic onsets compiled between 1997 and 2017 and achieves ~75% precision and recall rates. Furthermore, we find that IMF Bz and solar wind velocity (Vx) have the most significant influence on model performance and thereby provide maximum predictive power. Finally, we use principal component analysis to visually show a great degree of overlap between the solar wind and IMF characteristics of substorm and non-substorm intervals. This overlap suggests that solar wind and IMF alone may not provide sufficient information to clearly distinguish between these two classes and perhaps additional details about the dynamics of the magnetotail might be necessary to further improve the prediction accuracy.

DATA06 - Response of cosmic noise absorption to electron precipitation: A data-assimilation approach - by Adam Kellerman

Status of First Author: Non-student PhD

Authors: Adam C. Kellerman

Abstract: A data-assimilative approach is used to estimate electron precipitation into the atmosphere above several riometer stations over an 8-year period. The relationship between the precipitating electrons and cosmic-noise absorption is presented. A 2-D data-assimilative and quasi-linear diffusion model of the trapped electron particle population is employed to assimilate magnetospheric trapped electron observations from THEMIS, GOES, and the Van Allen Probes. The model then estimates transport of the electrons into the upper atmosphere. Empirical models of MLT-, L- and geomagnetic-activity-dependent wave power drive pitch angle and momentum diffusion in the code. For each event, and at each time step, estimates on non-adiabatic loss of electrons to the atmosphere are computed using a height-dependent loss-cone threshold, and a loss timescale of a quarter-bounce period. The results are presented in the form of statistics, and an empirical model relating CNA to precipitating electron flux.

DATA07 - Feasibility studies of global-scale airglow radiance data assimilation with GOLD observations - by Clayton Cantrall

Status of First Author: Student IN poster competition Masters

Authors: Clayton Cantrall, Tomoko Matsuo

Abstract: Far ultraviolet observations of Earth's airglow by the NASA Global-scale Observations of the Limb and Disk (GOLD) mission presents an unparalleled opportunity for upper atmosphere data assimilation. Assimilation of the GOLD observations can be formulated in a similar fashion to lower atmosphere radiance data assimilation approaches. To demonstrate such an approach, we present an implementation of an ensemble filter measurement update step using ensemble simulation of the thermosphere and far ultraviolet emission by the NOAA's Whole Atmosphere Model (WAM) and NCAR's Global Airglow model. The synthetic GOLD far ultraviolet disk emission data correspond to the GOLD Level 1C radiance data product. Observation system simulation experiments (OSSEs) test the feasibility of estimating three dimensional structure of thermospheric temperature, wind, and composition through assimilation of these GOLD Level 1C data. Thus far, the OSSEs have produced the following findings for temperature: (1) Assimilation of GOLD LBH disk emission data can reduce the modeled temperature biases by 97% under geomagnetically quiet conditions and 87% under disturbed conditions, and (2) The reduction in model uncertainty of temperature as a result of GOLD assimilation is 20% in the lower thermosphere and 25% in the upper thermosphere. The sensitivity of GOLD observations to wind and composition structure will also be tested. A radiance data assimilation approach such as the one presented here can extend the utility of GOLD observations to reveal global, time-dependent, vertically-resolved thermospheric structure, offering the key to addressing a number of outstanding questions including those relating to the properties of traveling atmospheric disturbances.

DATA08 - Investigation of thermospheric composition and dynamics using GOLD satellite mission: A data assimilation approach - by Fazlul Laskar

Status of First Author: Non-student PhD

Authors: Richard Eastes, Mihail Codrescu, Nicholas Pedatella

Abstract: The Global-scale Observations of the Limb and Disk (GOLD) mission can provide intensities of far ultraviolet emissions from Earth's atmosphere. From the spectral measurement of these emissions onboard the geo-stationary orbit, the composition and thermal state of the atmosphere can be retrieved at unprecedented temporal and spatial resolution. Those measurements will be used in an ensemble Kalman filter assimilation scheme with a background general circulation model to improve the system energy input. We expect it to provide better model results and information about atmospheric parameters other than those measured by the GOLD satellite. From such investigation we envisage obtaining a better understanding of the ionosphere-thermosphere system and of the physical processes that are active during normal and disturbed space weather conditions.

DATA09 - Physics-based Nonlinear Filtering of Orbital Debris Tracking Data for Density Estimation and Prediction - by Shaylah Mutschler

Status of First Author: Student IN poster competition Masters

Authors: Penina Axelrad, Tomoko Matsuo, Eric Sutton

Abstract: A key requirement for accurate trajectory prediction and Space Situational Awareness (SSA) is knowledge of the non-conservative forces affecting space objects. These effects vary temporally and spatially and are primarily driven by the dynamical behavior of space weather. Existing SSA algorithms adjust space environment models based on observations of calibration satellites. However, lack of sufficient data and mismodeling of non-conservative forces can cause inaccuracies in space object motion prediction, especially for uncontrolled debris objects. On the other hand, the uncontrolled nature of debris objects can make them particularly sensitive to the variations in space weather. Our research takes advantage of this behavior by utilizing observations of debris objects to infer the space environment parameters controlling their motion. We explore rigorous and practically realizable means to utilize debris objects as passive, indirect sensors of the space environment. The focus is on atmospheric density for more accurate prediction of Low Earth Orbit (LEO) object motion. In our previous work, a Partially Orthogonal Ensemble Kalman Filter (POEnKF) was implemented to assimilate observations of multiple debris objects, and estimate atmospheric density in addition to the position and velocity of each debris object. In this work, a methodology is developed that aims to estimate forcing parameters of a physics-based space environment model to allow for improved density estimates and predictions. This tool consists of two filters within a closed-loop feedback system. The first filter utilizes debris object tracking data in the form of measurements collected from ground sensors to estimate acceleration due to atmospheric drag. A couple orbital periods of accumulated debris object data are assimilated and the resulting estimated accelerations, as well as time, position, and debris object information, are passed to the second filter. The second filter, an Ensemble Square Root Filter (EnSRF), estimates forcing parameters of a physics-based space environment model, the Thermosphere Ionosphere Electrodynamic General Circulation Model (TIE-GCM). TIE-GCM is used to generate an ensemble of forecast density in the filter. The density ensemble combined with corresponding debris object ballistic coefficients forms a predicted acceleration measurement. The EnSRF applies corrections to the ensemble of predicted acceleration measurements using the first filter's acceleration estimates as measurements. A prior ensemble is utilized to empirically determine the nonlinear relationship between acceleration measurements and forcing parameters, allowing for corresponding corrections to forcing parameters. Ensemble filters have typically been employed in high-dimensional non-linear geophysical applications, such as weather forecasting of atmosphere and ocean systems. However, in the framework proposed here, a Particle Filter (PF) also provides a viable option for the second stage filter. Because our approach effectively reduces the state dimension to only a small number of forcing parameters (N state elements), it becomes feasible to implement the necessary particle space of 10N particles. A comparison between the performance of an EnSRF and PF for the second filter will be presented to demonstrate the advantage of a fully nonlinear filter for this particular system. Our current approach assumes that the ballistic coefficients of debris objects are known to a reasonable accuracy. This assumption is based on the idea of initializing the ballistic coefficients with information from the High Accuracy Satellite Drag Model (HASDM), which is regularly used in operations for updated density estimates. To accomplish this, density information from HASDM, when available, will be combined with debris object measurements to infer debris object ballistic coefficients. The end goal is a data assimilation framework capable of tolerating high-dimensional systems with nonlinear dynamics and sparse observations of specific objects, while also leveraging a class of observations not typically utilized. While all observations provide some information, regardless of their uncertainty, the cost of particular observations may outweigh their information contribution. Therefore, we will investigate what measurements are most cost effective. These measurements are identified by type (range, azimuth, etc.), sensor location, measurement uncertainty, and also by debris object class/orbital regime. Overall, our tool is expected to improve atmospheric density estimates, which will allow for more accurate LEO object motion prediction.

DATA10 - Meridian Chain of Interferometers (MerCI): A new observational network for thermospheric winds spanning the American Sector - by Patrick Dandenault

Status of First Author: Non-student PhD

Authors: Patrick Dandenault (JHU/APL), John Noto (CPI), Robert Kerr (CPI), Qian Wu (NCAR/HAO)

Abstract: A ten-station coordinated array of optical interferometers, stretching along a magnetic meridian from Resolute Bay Canada to King Sejong Station Antarctica, has been proposed. This meridian chain of interferometers (hereafter, MerCI) provides thermospheric neutral wind and temperature measurements with unprecedented accuracy and procedural uniformity. The research purposes are advancing analytical and assimilative dynamic modeling of the ionosphere, thermosphere, magnetosphere system; improved operational Space Weather forecasting (a charge that is now data-starved); and the establishment of an easily accessed discovery science community resource. These goals are motivated by high contemporary instrument sensitivities allowing enhanced duty cycles, modern machine learning applications for remote instrument performance assessments and distributed instrument data mining, and ease of access through web-based instrument control and data collection. Modeling expertise and specific modeling initiatives are integrated into the plan, as are relationships to other community instruments that will greatly the basic research.

DATA11 - Quantify Uncertainty in Probabilistic Space Weather Forecasting Models - by Shibaji Chakraborty

Status of First Author: Student NOT in poster competition Masters

Authors: S. Chakraborty, S. K. Morley

Abstract: Space weather impacts various facets of our everyday life, from GPS navigation service accuracy to radiation dose on transpolar flights. Space weather effects at Earth are driven by a wide range of solar and solar wind phenomenologies. Geomagnetic storms, whose intensity are often described by a geomagnetic index (Kp), are a space weather phenomenon whose consequences can cost billions of dollars. Hence forecasting space weather is a significant challenge addressing the security of modern technology. Current operational forecasts of geomagnetic indices use empirically-derived coupling functions or computationally expensive physics models to forecast short-term Kp, and neural networks for the 3-to-12 hour ahead prediction. None of these methods provide error/uncertainty estimation associated with their forecast. For higher values of Kp, the accuracy of current methods reduces, and the models in use are unable to quantify the uncertainty associated with the prediction. This work aims to provide a Kp forecast for 3 hours with uncertainty bounds associated with each prediction. We will explore both parametric and non-parametric techniques to give a probabilistic Kp forecast and quantify the uncertainty. Critical factors in obtaining a good prediction include appropriate choices of model and training data. We used solar wind parameters to predict Kp. Using transformed solar wind parameters, historical Kp values and different transfer functions can increase the accuracy of the models. Our candidate models mainly use dynamic training sets to produce forecasts. By this, we used variable training windows to find the best-fitted model, providing insights about the solar wind parameters and solar cycle and how they affect the coupling to the geospace environment.

EQIT01 - On the electrodynamics of equatorial plasma depletions using measurements from the Swarm mission - by Juan Rodriguez-Zuluaga

Status of First Author: Student IN poster competition PhD

Authors: Juan Rodriguez-Zuluaga, Claudia Stolle, Yosuke Yamazaki, Hermann Lühr, Jorge L. Chau

Abstract: Advance in the knowledge of the electric current system and electromagnetic characteristics of equatorial plasma depletions (EPDs) is crucial to understanding, not just the evolution of EPDs but also the background ionosphere where they develop. By combining simultaneous high-resolution measurements from the ESA's Swarm constellation mission, we have been advanced the current understanding of the electrodynamics of EPDs in three ways. Using electron density, electric and magnetic field measurements across large-scale EPDs, we have found that: (1) The field-aligned Poynting flux associated with EPDs is mainly interhemispheric rather than anti-parallel about the magnetic equator as suggested by earlier studies. (2) The related interhemispheric field-aligned currents exhibit a distinct seasonal and longitudinal dependence associated with a hemispherical asymmetry of the Pedersen conductance. (3) The orientation of diamagnetic currents at the edges of EPDs revealed both low and high plasma pressures within EPDs relative to the ambient plasma. It corresponds to the first observational evidence of plasma pressure enhancements in regions of depleted plasma density in the ionosphere. These new findings represent a small step towards a broader understanding of the electrodynamics of EPDs and open new directions to further studies not just on large-scale EPDs but also on the small-scale structures within EPDs.

EQIT02 - First results of ionospheric tomography using the LISN network - by Marcos Inonan

Status of First Author: Student NOT in poster competition Masters

Authors: Marcos Inonan, Payman Arabshahi

Abstract: The Low-Latitude Ionosphere Sensor Network (LISN) is a distributed observatory located in the South American continent. Composed by 50 GPS dual frequency receivers, this facility observes measurements of total electron content (TEC), especially the enhancements that occur near midnight. Taking advantage of the large number of stations of this network, Computerized Tomography technique is used to study the electron density distribution of the low-latitude ionosphere, especially in the moments of sudden increases in TEC between sunset until past local midnight. Different techniques are applied to the reconstruction, Iterative methods like algebraic reconstruction technique (ART), multiplicative algebraic reconstruction technique (MART) and inverse problem approach like the Generalized Singular Value Decomposition (GSVD) are evaluated. Results show advantages and disadvantages. While iterative methods show satisfactory results for specific initial conditions, they do very poorly in other cases and inverse methods do a great job without the help of any initial guess, they are limited to the number of ray paths to determine the resolution of the image and it is a regular base since LISN collects TEC data every 30 seconds approximately.These initial results show that LISN can be used as a tomography network, expanding its potential to investigate complicated ionospheric density irregularities.

EQIT03 - First statistical study of blanketing sporadic E over Jicamarca Radio Observatory using image processing techniques and machine learning algorithms - by José Manuel Suclupe Osorio

Status of First Author: Student IN poster competition Undergraduate

Authors: José M. Suclupe Osorio, Edgardo E. Pacheco Josán, Percy J. Cóndor Patilongo, Luis D. Cárdenas Andrade.

Abstract: We report the results of the first statistical study of blanketing sporadic E (Esb) occurrence over the Jicamarca Radio Observatory using the Digital Portable Sounder (DPS)-4 Digisonde data from 1996 to 2018. We found Esb occurs mainly during the December solstice and also during minimum solar years. We observe the occurrence of Esb mainly between 0700 and 2000 LT with a peak at 1600 LT. Additionally, we proposed a new criterion to identify Esb events taken into account the normal tendency of the F-layer minimum frequency of ionogram echoes due mainly to absorbance of the D-region. Esb events could be classified as rare events, in low latitude regions, and equatorial electrojet echoes often overlap with Esb echoes. A common methodology to identify Esb events have been done visually. We developed an algorithm and implemented a software to identify Esb events using image processing techniques and machine learning algorithms getting a Sensitivity of 87% in its first version. Finally, we have compared Esb events identified in ionogramas of Digisonde DPS-4 with VIPIR ionosonde and observed that identification of Esb events depends on the characteristics of the ionosonde and we discuss their differences.

EQIT04 - First measurement from a Geostationary orbit of Equatorial Plasma Bubble (EPB) zonal drifts and expansion rates using GOLD data - by Deepak Karan

Status of First Author: Non-student PhD

Authors: Deepak K. Karan, S. L. England, Robert Daniell, Carlos Martinis, Richard Eastes, Alan G. Burns, and Bill McClintock

Abstract: A reduction of plasma density occurs after the sunset on the bottom-side of the F-region due to the Rayleigh-Taylor instability over the dip-equator. The depleted region of plasma grows to higher altitudes and gradually spreads to higher latitudes along the magnetic field lines. These depleted plasma density regions are referred to as the equatorial plasma bubbles (EPBs). Observations from the ground using ionosonde, GPS, and all sky imagers, as well as from space-based platforms using far-ultraviolet imagers have been carried out to track the movement of plasma bubbles. This allows us to understand the underlying processes that form night time plasma irregularities. However, measurements from space-based platforms are limited in temporal resolution, whereas ground-based measurements are limited in the spatial resolution. Global-scale studies of these phenomena are now possible using Far-Ultraviolet measurements obtained from geostationary orbit by the Global-scale Observations of the Limb and Disk (GOLD). The nighttime OI 135.6 nm emission obtained by GOLD are used to observe plasma bubbles continuously over the American, Atlantic, and African longitude sectors for the first time. These unique data sets are used to compare the zonal drifts and expansion rates of the plasma bubbles and their longitudinal variability. Using these data will enable us to address the underlying processes behind the occurrence of ESF and other equatorial plasma instabilities.

EQIT05 - Discrepancy in Mid-Afternoon Electron Temperatures Between Jicamarca ISR Data and SAMI Ionospheric Models - by Sevag Derghazarian

Status of First Author: Student IN poster competition Masters

Authors: Sevag Derghazarian, D. L. Hysell

Abstract: The plasmasphere is the layer of the Earth's atmosphere found immediately above the topside ionosphere, beginning at a height where the fractional composition of the H+ ion exceeds 50%, and continuing all the way up to the plasmapause. A thorough and more detailed characterization of this layer is of prime importance for a better understanding of our planet's space weather as well as our ability to improve existing upper atmospheric models. High altitude experiments at Jicamarca were designed to probe this region and the topside ionosphere in more detail, making use of the "Full Profile" signal processing technique which yields continuous estimates of electron density (Ne), electron, ion temperature (Te, Ti) and ion composition with altitude. A recent high altitude experiment was performed over Jicamarca in January of 2019. The experiment incorporated minor changes to the pulse transmission and data processing techniques which will be detailed in the poster. One of the peculiarities in the data is a mid-afternoon drop in Te, which is also a feature present in all of the previous experiments. This dip in Te, however, does not appear in ionospheric models (such as SAMI2, SAMI2-PE and SAMI3) and several likely explanations involving photoelectron transport are proposed and elaborated. Preliminary changes are incorporated into SAMI2-PE, in order to reproduce the midday Te drop. A new technique for correcting noise and lag product estimates calculated through order statistics will also be presented. It is incorporated into the "Full Profile" algorithm for better estimates. This technique was developed for use in Jicamarca ISR experiments, but could be of interest to any ISR experiment which involves contamination from coherent echoes.

EQIT06 - Study of equatorial ion drifts over the Jicamarca Radio Observatory - by Edgardo Pacheco

Status of First Author: Non-student PhD

Authors: Edgardo Pacheco, Percy Condor, Jose Suclupe, Josemaria Gomez, Fernando Villanueva

Abstract: Ion drifts at low latitudes play a key role in the physical processes and phenomena that occur in the ionosphere. Drift measurements improve significantly our understanding of the ionospheric electric fields that is a fundamental parameter in the complex interactions of the ionospheric electrodynamics. The understanding of the ion drift characteristics and sources of this variability is essential for improved ionospheric models and testing of predictions for space weather effects. We investigate the equatorial vertical ion drifts of the last solar cycle observed over the Peruvian sector by using 50 MHz incoherent scatter radar and JULIA radar measurements made at the Jicamarca Radio Observatory to describe the different characteristics during the mínimum and solar máximum periods. These observations are compared to those from previous cycles. Variations between season, local time are also examined. In addition, ionograms and TEC measurements from 2016 to 2018 will be utilized to complement the observations and illustrate the behavior of the ionosphere on particular cases.

EQIT07 - Estimating the daytime vertical ExB drift velocities in the F-region of the equatorial ionosphere using the IEEY and AMBER magnetic data in West Africa - by Kassamba Abdel Aziz Diaby

Status of First Author: Student IN poster competition Masters

Authors: Olivier Kouadio Obrou, Vafi Doumbia

Abstract: In this paper the daytime vertical E×B drift velocity in the F-region of the equatorial ionosphere was estimated from the magnetic effect of the equatorial electrojet (EEJ) in the West African longitude sector. In this purpose, the geomagnetic data recorded during the International Equatorial Electrojet Year (IEEY) from 1993 to 1994 and that provided in 2013 by the African Meridian B-field Education and Research (AMBER) network were used. For the IEEY project, data from Sikasso (11.34° N, 5.71° W, 0.12°diplat), Tombouctou (16.73° N, 3° W, 6.76 diplat) and Lamto (6.23° N, 5.02° W, -6.27 diplat) were considered. For the AMBER project data from Conakry (10.5°N, 13.71°W, -2.69°diplat) and Abidjan (4.60° N, 6.64° W, -8.54° dip) were considered. The vertical drift velocity was inferred from the EEJ contribution (ΔH) in the geomagnetic field horizontal component. The estimated noontime seasonal averages are respectively Vd=10.95m/s and Vd=9.46m/s for March and September equinoxes; Vd= 8.75 m/s and Vd=8.27 m/s for December and June solstices. The daytime vertical drift velocity was found to be larger in equinoxes than in solstices. These values are in agreement with the results of previous studies in the same longitude sector.

EQIT08 - The Kiritimati Equatorial Ionospheric Observatory (KEIO) Project - by Louise Gentile

Status of First Author: Non-student Masters

Authors: R. T. Parris, T. R. Pedersen, E. V. Dao, K. S. Obenberger, J. M. Holmes, L. C. Gentile, J. Hines, R. Kelly, Z. Balint, K. Robinson, J. J. Moses, S. Kumar

Abstract: A new SuperDARN style radar is planned in the equatorial zone, as the cornerstone instrument of the Kiritimati Equatorial Ionospheric Observatory (KEIO) on Christmas Island, Kiribati. This new radar is expected to observe field aligned irregularities associated with equatorial plasma bubbles, the equatorial electrojet, and 150km echoes over very long oblique ranges, as well as to monitor HF propagation conditions.
In partnership with AFOSR and the University of the South Pacific (USP), who will operate the new facility, a site has been proposed on Kiritimati, Kiribati. This new observatory, which will house a future USP teaching and research center, will eventually host GPS scintillation and TEC receivers, a LEO beacon receiver, UHF scintillation receivers, all-sky optics, and VLF receivers.

EQIT09 - Ionospheric effects near the EIA crest under extreme space weather conditions - by Debasis Jana

Status of First Author: Student IN poster competition Masters

Authors: Debasis Jana, Shyamal Kumar Chakraborty

Abstract: Ionospheric responses to geomagnetic storms are manifested by drastic modifications of dynamics, electrodynamics and neutral composition of the earth's atmosphere-ionosphere system on a global scale. The resulting disturbances in the ionospheric parameters are the mixture of several solar terrestrial processes. Since no two ionospheric storms are quite the same, it is desirable to make a comprehensive study on the evolution of ionospheric effects under several geomagnetic storm conditions. Under present investigation an extensive study on the variability of occurrences of ionospheric scintillation at Raja Peary Mohan College (22.65°N, 88.36°E) located near the EIA crest and GNSS total electron content (TEC) during the periods of 13 intense (Dst< -100 nT) geomagnetic storm distributed over the 5 years' period of 2011-2015 has been made. The study is augmented with electrojet data collected from wdc, IIGMumbai and neutral composition data obtained from GUVI satellite images. IGS TEC data at Port Blair (11.3ON, 92.4OE), IISC Bangalore (13.0ON, 77.3OE), Lucknow (26.5ON, 80.5OE), Cocos (12.1OS, 96.5OE) and Diego Garcia Island (7.1OS, 72.2OE) available with www.igs.org are also investigated for the study. Out of total 13 storm events 8 storms occurs in equinoctial months, 3in summer and 2 in winter months respectively. The main phase occurrence times are distributed on pre-noon, around sunset and post-midnight periods respectively. Both the positive and negative storm effects are reflected in TEC variability and in few cases opposite features are prominent in small longitude separation (~5O). Occurrence of scintillation seems to deviate from the climatological pattern reported till date. The observation may be explained in terms of electric field modulation under different stages of the particular space weather event. The contribution of neutral composition changes are found to be important to explain the variability patterns of ambient ionization. The variation of interplanetary parameters as well as subsequent magnetosphere ionosphere coupling process may be attributed to the variability of ionospheric parameters. Observations reveals that dominating mechanisms are changing in different phases of storm and importance of the respective process changes from storm to storm.

EQIT10 - Multi-instrument observations of super equatorial plasma bubbles over American and Asian sectors - by Ercha Aa

Status of First Author: Non-student PhD

Authors: Ercha Aa, Shasha Zou, Aaron Ridley, A. J. Coster, Shunrong Zhang

Abstract: This paper presents observations of super equatorial plasma bubbles (EPBs) occurred at local dusktime both in American and Asian sectors during a storm on 8 September 2017. The main features and spatial-temporal evolution of EPBs are studied and can be summarized as follows: (1) channel-like structures of GNSS TEC depletion that occurred simultaneously at geomagnetically conjugate points, (2) significant equatorial and midlatitudinal electron density (Ne) bite-outs measured by Defense Meteorological Satellite Program (DMSP) and Swarm satellites, and (3) poleward extension of bubble-related ionospheric irregularities/depletions along the magnetic field lines. One prominent feature is that the EPBs-related depletions reached very high magnetic latitudes (MLAT: 46o), which could map to an apex altitude of 6,800 km over the magnetic equator. In addition, the plasma depletions over North America merged with the wavy structures of large-scale TIDs; while the plasma depletions over Asian sector have relatively large westward tilt angle with respect to the field lines.

EQIT11 - Statistical analysis of equatorial plasma irregularities retrieved from Swarm 2013--2019 observations - by Ercha Aa

Status of First Author: Non-student PhD

Authors: Ercha Aa, Shasha Zou

Abstract: In this study, we present a statistical analysis of equatorial plasma irregularities (EPIs) by using in situ plasma density measurements of Swarm constellation from December 2013 to February 2019, the second half of the solar cycle 24. The occurrence probability and associated temporal/spatial distribution patterns with respect to longitude, season, local time, latitude, solar activity, and geomagnetic activity are investigated, respectively. The main results are as follows: (1) The longitudinal distribution of equatorial plasma irregularities has maximum values around the South American-Atlantic-African sectors. (2) There are asymmetrical seasonal variation of the occurrence rates. The occurrence rates in the South American (African-Pacific) sector have higher values around December (June) solstice, while occurrence rates over the Atlantic and other sectors usually reach maximum values during equinoctial periods. (3) The occurrence pattern of EPIs significantly varies with local time. (4) The occurrence rates have certain dependence on geomagnetic activity to some extent but the correlation with solar activity is complicated. The possible mechanisms for the above finding are discussed correspondingly.

EQIT12 - On the magnitude and variability of height gradients in the equatorial F-region vertical plasma drifts - by Samuel Shidler

Status of First Author: Student IN poster competition Masters

Authors: Sam Shidler, Fabiano Rodrigues

Abstract: Previous radar studies have shown that magnitude of the vertical component of equatorial ionospheric $\bf{E} \times \bf{B}$ plasma drifts can vary significantly with height, even within main F-region altitudes. These studies, however, were limited to few observation days.
In order to properly quantify the height variation of equatorial F-region vertical drifts, we examined 559 days of measurements made by the incoherent scatter radar (ISR) of the Jicamarca Radio Observatory (JRO) between the years of 1986 and 2017. From the observed profiles of vertical plasma drifts, we determined the mean behavior and variability of the height gradients as a function of local time and two distinct solar flux conditions (mean $F_{10.7}$ around 80 and 150 SFU). Only observations made under geomagnetically quiet conditions were considered. Our results quantify the enhanced negative height gradients of vertical drifts near sunset that have been reported in the past. More importantly, we also identify and explain an enhancement in positive gradients near sunrise. We discuss the variability of the height gradients in vertical ionospheric $\bf{E} \times \bf{B}$ drifts at main equatorial F-region heights, and the impact of this variability for satellite observations and studies of ionospheric stability and equatorial spread F.

EQIT13 - Electrodynamics of the low latitude ionosphere during September 6-9 2017 - by Anastasia Newheart

Status of First Author: Student IN poster competition Masters

Authors: A. Newheart, S. Sazykin, A. J. Coster, V. Coffey, M. Chandler, B. Fejer, P. J. Erickson, L. Navarro

Abstract: The geomagnetic storm of September 7-9, 2017 occurred during an interval of enhanced solar activity resulting in multiple flares, several coronal mass ejections (CMEs), and a number of space weather-related phenomena. . Although the minimum value of the Dst index reached only ~150 nT, the storm resulted in disruptions of high frequency radio communications. This paper uses multi-instrument observations of the ionospheric F-region densities and electric fields to characterize the storm-time response to the magnetospheric disturbance and compares the storm-time behavior to the quiet day before the storm. We use in situ F-region (~400 km altitude) ion densities measured by the FPMU instrument suite on board the International Space Station (ISS), global maps of the total electron content (TEC) derived from ground-based GPS receivers, and incoherent radar measurements from the Jicamarca Radio Observatory (near the magnetic equator) and from the Millstone Hill incoherent scatter data. Our analysis shows that the ionospheric response near local midnight (between 20 and 02 local time) is the most pronounced in the American longitudinal sector, where both in situ density data and TEC maps indicate significant enhancements. We associate these density peaks with the storm-time Appleton anomaly that extends to late local times. We will also present observations of significant plasma density depletions and irregularities in the FPMU data near the equator in the post sunset region that are interpreted as arising from spread-F type instabilities. The dependence of these irregularities will be analyzed in terms of their local time and storm phase. We compare the FPMU measurements to measurements from the Swarm and DMSP satellites during the same time period. Finally, we will use incoherent scatter measurements (including ExB ion drift velocities) to place these results in the context of storm-time electrodynamics.

EQIT14 - The Role of the Thermospheric Winds on the EIA and PRE Measured by the SOFDI Instrument at the Geomagnetic Equatorial Latitudes - by Sovit Khadka

Status of First Author: Non-student PhD

Authors: Sovit Khadka, A. Gerrard, C. Valladares, E. Vidal-Safor, M. Milla, O. Veliz, J. Chau, and J. Meriwether

Abstract: Second-generation, Optimized, Fabry-Perot Doppler Imager (SOFDI), a triple-etalon Fabry-Perot interferometer, is designed to make 24-hour measurements of thermospheric winds from OI 630-nm emission. We present both night and day thermospheric wind observations made over the recent years using SOFDI at American low latitudes. These results were obtained from under the geomagnetic equator at Huancayo, Peru during the summer 2011-2018 periods and are compared to the equatorial ionization anomaly (EIA) derived from GPS-TEC and Jicamarca incoherent scatter radar (ISR) measurements of the pre-reversal enhancement (PRE). We report i) the dynamics of the EIA asymmetry, ii) the climatology of the summer winds above Huancyao, iii) the direct relationship between the afternoon winds and the magnitude of the PRE, and iv) the large variability seen in the afternoon winds, which are likely caused by synoptic tidal activity modulating gravity waves. These results confirm the role that the thermospheric winds play in modulating equatorial dynamics, and further demonstrate the need for both zonal and meridional components of the wind flow.

EQIT15 - A fast implementation on Deconvolution and full-profile inversion of ionospheric radar data from Arecibo Observatory - by Binghui Wang

Status of First Author: Student IN poster competition Masters

Authors: Binghui Wang

Abstract: Incoherent scatter radar (ISR) can be used to estimate key ionospheric state parameters such as electron density, ion composition, electron and ion temperature. Different types radar pulsing techniques can be chosen to establish some type of a compromise between height and frequency resolution. Typically in "long pulse" mode, there is a range smearing issue caused by superposition of multiple returns. One of the approaches to solve this is proposed [Nikoukar et al., 2008] using inversion methodology. This work focuses on implementing Nikoukar's approach in a practical and computation efficient scheme using Cholesky factorization. The new implementation is 20 times faster than the traditional method using Conjugate Gradient

EQIT16 - Geomagnetically Induced Currents (GICs) related to impulsive Space Weather events at Low Latitudes. - by N'Guessan Kouassi

Status of First Author: Student IN poster competition PhD

Authors: Vafi Doumbia, KOUADIO BOKA ,ZIE TUO

Abstract: Geomagnetically induced currents (GICs) regularly damage the technological infrastructures in high latitude regions. Its effects have also been observed in middle and low latitudes (South Africa, China.) (Gaunt and Coetzee, 2007). In view of these dangers, we study the GICs at low latitudes in order to determine the level of induction associated to the solar events which are the cause of these induced currents. We estimate GIC intensity by two methods. Firstly, we use measured geoelectric data to infer GIC and secondly, we calculate geoelectric field data by geomagnetic field data and infer GIC.

ITMA01 - Observations for aurora and relevant polar upper atmospheric changes at Jang Bogo station, Antarctica - by Young-bae Ham

Status of First Author: Student IN poster competition student

Authors: Young-bae Ham, Geonhwa Jee, Changsup Lee, Hyuckjin Kwon, Eunsol Kim

Abstract: We have been collecting aurora images from color-CCD All-Sky Camera (ASC) at Jang Bogo Station (JBS), Antarctica (74° 37' S, 164° 13' E) since 2018. The JBS is located mostly in the boundary between the polar cap and the auroral region and since the establishment in 2014, various observations for the polar upper atmosphere and the magnetosphere have been performed simultaneously together with the auroral observation. In this study, we analyze the 1-year observation for the aurora as well as the polar upper atmosphere and the magnetosphere from the various ground instruments such as ionosonde (VIPIR), Febry-Perot interferometer (FPI), magnetometers, and ASCs in order to study on the possible changes of the polar upper atmosphere during the occurrence of the aurora over the JBS. In this presentation, we will show some preliminary results of this comparative study mainly using the auroral images from ASC and the simultaneous observations for the ionosphere and the thermosphere.

ITMA02 - A multi-static meteor radar at Andes Lidar Observatory - by Zishun Qiao

Status of First Author: Student IN poster competition PhD

Authors: Zishun Qiao, Alan Liu

Abstract: With the support of an NSF MRI grant, a multi-static meteor radar will be installed around Andes Lidar Observatory in Cerro Pachón, Chile (30.3S, 70.7W, ALO). The main transmitter will be at ALO, and two remote stations at Las Campanas Observatory 137 km to the north and Southern Cross Observatory 108 km to the south. This system will provide 24-hr continuous horizontal wind measurement in a region where mountain waves are frequently generated. Together with the Na wind-temperature lidar and airglow imagers at ALO, they provide comprehensive measurements of the MLT atmosphere at a broad range of spatial and temporal scales. The details of the instrument, deployment sites, and expected data product will be presented.

LTVI01 - Calibrating Atomic Oxygen Ion Profiles Retrieved from Ground-based observations of 630.0 nm Airglow Intensity - by Yi Duann

Status of First Author: Student IN poster competition PhD

Authors: Yi Duann, Loren C. Chang, Yi-Chung Chiu, Alexei V. Dmitriev, Konstantin G. Ratovsky, Irina V. Medvedeva and A. V. Mikhalev

Abstract: When the atomic oxygen ions distributed in the ionospheric F region experience an energy level transition, visible light with a wavelength of 630 nm is released. As such, 630 nm airglow emission intensities are proportionate to the density of atomic oxygen ions ([O+]) that dominate the composition of the F region, and measurement of these emissions is an attractive option for passive monitoring of F layer variability. In a previous study, we derived photochemical inversion models based on the formulas derived from the theories of R. Link and L. L. Cogger (1988), Sobral et al. (1993), and Vladislav Yu. Khomich et al. [2008]. hmF2 was used as a parameter for applying a Gaussian Distribution to approximate the vertical profile of [O+], which resulted in overestimation of [O+]. In this research, the peak height is calibrated to a more reasonable region with a new height assumption according to past observations. (Y. Otsuka et al. 2003). For self-consistency, the Thermosphere Ionosphere Electrodynamic General Circulation Model (TIEGCM) was selected for the purpose of testing and calibrating the photochemical inversion models. With the ions and neutral particle values produced by same data source, the potential possibility of introducing errors through the use of multiple non-consistent empirical models is decreased. The airglow intensity measured by airglow spectrometer observations from the Geophysical Observatory of the Siberian Branch of the Russian Academy of Sciences near Irkutsk, Russia (51.8°N, 103.1°E), is compared to the electron density and atomic oxygen ion density calculated by the TIE-GCM model and our self-developed photochemical inversion models at 250 km, which is close to the altitude of the 630.0 nm airglow layer. With the new calibration and optimization, our self-developed photochemical inversion models could offer more promising results using empirical models and airglow intensity in the future.

LTVI02 - Infrared Radiation in the Thermosphere: Solar Cycles 19-24 and the Approach to Solar Cycle 25 - by Linda Hunt

Status of First Author: Non-student Masters

Authors: Linda Hunt, Marty Mlynczak, B. T. Marshall, James R. Russell III

Abstract: Observations of thermospheric infrared radiative cooling by carbon dioxide (CO2) and nitric oxide (NO) derived from measurements made by the Sounding of the Atmosphere using Broadband Emission Radiometry (SABER) instrument on the Thermosphere-Ionosphere-Mesosphere Energetics and Dynamics (TIMED) satellite from 2002 to present will be shown. The time span of these measurements covers more than 6,300 days including much of solar cycle (SC) 23 and the entirety of SC 24 to date. This set of thermospheric cooling has been extended back to the year 1947 via the Thermosphere Climate Indexes, providing quantitative measures of the effects of solar variability on the terrestrial atmosphere in the current solar cycle and its five predecessors. Maxima of infrared cooling rate profiles (nW/m3) are smaller during SC 24 than SC 23, indicating a cooler thermosphere. Rates of global infrared power (W) from CO2 are now at levels observed during the deep solar minimum of 2009. Rates of NO power are still larger than those observed during 2009 and are being maintained at an elevated level by geomagnetic activity. During SC 24 to date, the thermosphere has radiated less than 75% of the energy of the mean of the past five cycles. At current infrared radiation levels, SC 24 would have to extend another 1500 days, or more than 4 years, to equal the mean integrated infrared power of the five preceding solar cycles. Meanwhile, forecasts for SC 25 predict another long, deep solar minimum with its nadir occurring sometime between July 2019 and September 2020, so SC 24's integrated power would not reach the previous five-cycle mean.

LTVI03 - Newly derived thermospheric products for CHAMP, GRACE, GOCE and Swarm - by Günther March

Status of First Author: Student IN poster competition Masters

Authors: G. March, T. Visser, E. Doornbos, P.N.A.M. Visser, J. van Den IJssel, E. Iorfida

Abstract: The CHAMP, GRACE, GOCE and Swarm satellites have been very productive to improve the understanding of atmospheric dynamics and coupling processes in the thermosphere-ionosphere region. Accelerometers and GPS-receivers on board of these satellites provided, and are providing, high-resolution thermosphere products. Within satellite data, so far, scale differences with empirical models have been largely neglected or removed using ad hoc scale factors. The source of these differences arises from errors in the satellite geometry, aerodynamics and gas-surface interactions (GSI) modelling. Previously used simplified models could not provide high-fidelity information about satellite outer surfaces and energy exchanges between atmospheric particles and satellites. Within this study, an enhanced geometry and aerodynamic modelling with a better characterization of gas-surface interactions aims to reduce these uncertainties. The satellite accelerations have been reprocessed using newly estimated GSI parameters leading to high-fidelity density and wind estimates. Long periods and attitude manoeuvres have been investigated in order to provide an overview of GSI modelling influence and the associated thermospheric products sensitivity. In this work, the improved densities and winds are presented and compared with empirical atmospheric models. The presented improved products are expected to be useful to the thermosphere-ionosphere science community to further increase the understanding of atmospheric dynamics, space weather and long trends.

LTVI04 - What Whole Atmophere Model Time Slice Simulations Tell Us About Thermosphere/Ionosphere Multi-Decadal Changes from the 1920s to 2010s - by Joe McInerney

Status of First Author: Non-student Masters

Authors: Joe McInerney, Stan Solomon, Liying Qian, Hanli Liu, Francis Vitt, Jing Liu

Abstract: Time slice free running simulations were performed for the time period from the 1920s to 2010s using the The Whole Atmosphere Community Climate Model -eXtended (WACCM-X). The changes in a number of model output fields were examined in the atmosphere above 100 kilometers. Here we present the basic characteristics of thermosphere/ionopshere changes during this 90-year time period.

LTVI05 - Neutral Temperature Change caused by Secular Changes of Geomagnetic Fields in the Whole Atmosphere Region - by Xu Zhou

Status of First Author: Student IN poster competition Undergraduate (checking)

Authors: Xu Zhou, Xinan Yue, Hanli Liu, Weixing Wan, Yongxin Pan, Joseph Mclnerney

Abstract: This work performs several simulations to evaluate temperature changes caused by secular changes of geomagnetic fields (SCFG) and increase of anthropogenic emissions and to estimate contribution of SCGF to the total climate temperature changes in the entire atmosphere during past 35 years, based on the Whole Atmosphere Community Climate Model-eXtended (WACCM-X) v2.1. The results shows SCGF has no obvious contribution to the global mean temperature, but it causes a significant warming (cooling) in the Arctic (North American) in the thermosphere. Below ~130 km, SCGF hardly affects climate temperature significantly. Besides, climate temperature changes has apparent local time dependence, and the contribution of SCGF becomes largest at 15 LT. Overall, this work indicates the ability of WACCM-X v2.1 to describe climate change driven by different sources and give a comprehensive understanding about climate temperature changes caused by SCGF.

LTVI06 - Influence of Lower Thermospheric Circulation on Semi-Annual Oscillation in the Ionosphere and Thermosphere using GITM, MSIS and WACCM-X - by Garima Malhotra

Status of First Author: Student IN poster competition PhD

Authors: Aaron Ridley, Daniel R. Marsh, Larry Paxton

Abstract: Semi-Annual oscillation (SAO) is one of the dominant long-term variations in the thermospheric and ionospheric densities. The upper atmospheric sources that contribute to it, such as, thermospheric spoon mechanism, geomagnetic activity have been investigated in many previous studies. However, the role of lower atmosphere, such as tidal mixing, gravity wave mixing, lower thermospheric residual circulation on SAO is still under investigation. Global Ionosphere Thermosphere Model (GITM) in its default configuration uses MSIS as the lower boundary which has lower atomic oxygen densities in summer and higher in winter at 98 km (similar to thermospheric spoon). However, in this study, we analyze the effect of changing the lower boundary of GITM to WACCM-X which has opposite latitudinal gradient

in atomic oxygen densities, higher in summer and lower in winter (also called as lower thermospheric residual circulation) at 98 km. We also compare these with the baseline simulation, MSIS with no SAO at the lower boundary to find the relative contribution of lower vs upper atmosphere to SAO. We analyze the latitudinal and global magnitudes of the SAO, the meridional and vertical transport in the thermosphere and the effect on TEC, O/N2, NmF2 and neutral densities and compare the simulation results with data such as GPS, GUVI, COSMIC and GRACE. We also compare the SAO amplitudes for each of the simulations between solar maximum and solar minimum years. We find better agreement with the data during solstices when using WACCM-X densities. However, during equinoxes, we did not see any improvement in the model-data agreement.

LTVM01 - Solar Cycle Implications in Nine Years (2010 - 2019) of Polar Mesospheric Clouds over McMurdo, Antarctica - by Manuel da Costa Lindo

Status of First Author: Student IN poster competition Undergraduate

Authors: Mattia Astarita, Zimu Li, Ian Geraghty, and Xinzhao Chu

Abstract: The Polar Mesospheric Clouds (PMC) measurements can help us understand better how the solar cycle can impact our upper and middle atmosphere. It can also provide an important tracer to monitor the climate change in this region, and study atmospheric dynamics. This project aims to analyze the PMC data collected from a Fe Boltzmann temperature lidar, located at Arrival Heights (77.84S, 166.67E) near McMurdo, Antarctica and operated by the University of Colorado at Boulder. The lidar team has managed to collect data continuously for 9 seasons, beginning in December 2010. These consecutive years of data allow us to register the main characteristics of Polar Mesospheric Clouds, as well as their occurrence in this latitude. The aim of this endeavor is to analyze the data from December 2010 to February 2019. The months registered will include November, December, January, and February. The main aspects to be studied under these conditions include inter-annual, seasonal, diurnal variations to PMC conditions and, afterward, extrapolate significant behavior. It will try to build upon Chu et al. [2003], [2006], and [2011] to consolidate data and identify some possible Solar Cycle relationship. The long-term goal is to use the PMC data to see if some characteristic patterns match up the solar radiation variations over a solar cycle. The data will encapsulate almost the entirety of a full solar cycle, which usually lasts 11 years. It will be an accurate depiction of the different stages of such cycle which shows a steady increase from a minimum in 2010 to a maximum in 2014 and a consequent decline in sunspot numbers since then. These spots are locations of intense solar activity and emit more radiation than the average Sun's surface. We are also looking to confirm the relationship established by Chu et al. [2011] and Astarita et al. [2017].

METR01 - New Meteor Radar at Poker Flat Research Range: First Observations and Analysis - by Jared Klemm

Status of First Author: Student IN poster competition Master (checked)

Authors: Jared Klemm, Jennifer Alspach, Jintai Li, Denise Thorsen, Richard Collins, Katrina Bossert, Biff Williams

Abstract: In November 2018, the researchers at the University of Alaska Fairbanks installed a monostatic meteor radar system at Poker Flat Research Range. The primary goal is to extend the scope of current studies in the Arctic by combining radar and lidar wind, temperature, and density measurements. The co-location of the newly installed meteor radar with a Rayleigh lidar system and a sodium resonance wind-

temperature lidar (SRWTL) system at Poker Flat Research Range allows for measurement of ambient temperature and density across the meteor region (75-100km). This poster presents some "first light" results from the radar, including typical daily meteor counts and distributions. Also presented in this poster is a preliminary analysis of ambient temperature and density comparisons between the radar and both lidar systems. There is a model relationship between temperature, density, and ambipolar diffusion coefficient that allows for one of these parameters to be calculated when the other two are known. In this study, independent measurements from the three systems are used to assess the self-consistency of the model relationship. Density is calculated using ambipolar diffusion coefficient from the radar and temperature from the SRWTL, then compared to the ambient density from the Rayleigh lidar. Similarly, temperature is calculated using ambipolar diffusion coefficient from the radar and density from the Rayleigh lidar, then compared to the temperature measured by the SRWTL.

METR03 - Sparse meteor signal recovery from MIMO radar measurements - by Juan Urco

Status of First Author: Student IN poster competition Masters

Authors: J. M. Urco, J. L. Chau, T. Weber, J. Vierinen

Abstract: Since the 1950s, specular meteor radars (SMRs) have been used to study the mesosphere and lower thermosphere (MLT) dynamic. Atmospheric parameters derived from SMRs are highly dependent on the number of detected meteors and the accuracy of meteor's location. Recently, we have proposed the use of incoherent and coherent multiple-input-multiple-output (MIMO) radar approaches combined with spread spectrum to increase the number of detected meteors and to extend the altitude and horizontal coverage. The incoherent MIMO approach refers to the addition of new transmit sites (widely separated), whereas the coherent MIMO refers to the addition of new transmit antennas in the same site (closely separated), in both cases, transmitting a different pseudo-random sequence from each antenna element. Unfortunately, the addition of new transmit antennas with different code sequences degrades the performance of conventional signal recovery algorithms. This as a consequence of the cross-interference between the transmitted signals, making it worse as the number of transmitters increase. In this work, we propose a novel signal recovery approach based on Compressed Sensing, taking advantage of the sparse nature of meteor echos. The approach allows exact recovery of weak echos even in interference environments. Besides the advantage of the proposed approach to recover the meteor signal, we will discuss the optimal selection of the transmitted codes and the minimum code length required for exact recovery. Additionally, we propose a modification of the Orthogonal Matching Pursuit (OMP) algorithm used in sparse problems to make it applicable in real-time analysis of large data. The success of the proposed approach is corroborated using Montecarlo simulations and real data from a meteor radar network installed in northern Germany.

MLTG01 - Statistical characterization of high-to-medium frequency gravity waves by WACCM-measured vertical winds and temperatures in the MLT - by Yu Wang

Status of First Author: Student IN poster competition master (checked)

Authors: Yu Wang, Xian Lu

Abstract: We present the study of gravity waves with periods of 0.5-2.7h and wavelengths of 5-60 km that are dominant in the vertical winds and temperatures measured by the UCAR in Boulder, CO (40.1°N,105.2°W). The ratio of these two wave amplitudes, probability density functions of these two amplitudes, phase differences and vertical wavelengths are derived from the observations basically using 2-D wavelet transforms. The phase differences between the vertical winds and temperatures (φ_W-φ_T) follow a Gaussian distribution with 90.3±31.2°. The amplitude ratios are positively correlated with the ground-based periods with a coefficient of ~0.29. We will use the wavelengths derived from horizontal comparing with the periods & wavelengths we already got vertically.

MLTG02 - Gravity Wave Activities in the Upper Mesosphere Observed at King Sejong Station, Antarctica (62.22°S, 58.78°W) and Their Potential Sources in the Lower Atmosphere - by Byeong-Gwon Song

Status of First Author: Non-student Undergraduate

Authors: Byeong-Gwon Song, In-Sun Song, Hye-Yeong Chun, Changsup Lee

Abstract: Gravity wave (GW) activities in the upper mesosphere and their potential sources in the lower atmosphere are investigated using meteor radar observations at King Sejong Station, Antarctica (KSS; 62.22°S, 58.78°W) for 8 years (2007–2014). GW activities are estimated through hourly GW wind variances obtained from an improved methodology that explicitly removes large-scale wind components (including tides and planetary waves such as 2- and 4-day waves) from observed meteor echoes. A clear semi-annual variation of the GW activities with solstitial maxima and equinoctial minima exists, except above 94 km where GW activities are strong in August–September. Potential GW sources in the lower atmosphere, including orography, jet stream, and deep convection, are investigated using reanalysis datasets. Orography around KSS is a likely source of GWs in winter and autumn, as stationary mountain waves can propagate up into the upper mesosphere without being filtered by the westerlies from the surface to the upper mesosphere. The residual of the nonlinear balance equation at 5 hPa, which is a diagnostic of flow imbalance associated with the polar night jet (PNJ), significantly correlate with the observed GW activities at $z = 98$ km during spring and autumn, while no significant correlation is found in wintertime due to critical-level filtering and Doppler shifting via the strong PNJ. Deep convection at midlatitudes is a likely source of the GWs in nearly all seasons, with the strongest correlation in storm tracks in winter.

MLTG03 - Characterization of line-of-sight effects in gravity waves as observed in the stratosphere, mesosphere and thermosphere-ionosphere - by Jaime Aguilar Guerrero

Status of First Author: Student IN poster competition PhD

Authors: Jonathan Snively, Christopher Heale, Pavel Inchin, Matthew Zettergren

Abstract: Gravity waves (GWs) are major drivers of the upper atmosphere circulation [e.g., Fritts and Alexander, RG, 41, 2003]. Convectively generated GWs, which are often concentric about their sources, can have sufficiently large vertical wavelengths and horizontal phase speeds to significantly affect multiple layers of the atmosphere [e.g., Taylor and Hapgood, PSS, 36(10), 1988; Yue et al., JGR, 114, 2009; Nishioka et al., GRL, 40, 2013]. With modern capabilities for remote sensing different layers of the atmosphere it is now possible to calculate GW parameters at different altitudes for particular events or sources [e.g., Yue et al., JGR, 118, 2013; Akiya et al., GRL, 41, 2014; Azeem et al., GRL, 42, 2015]. By performing simulation studies, especially when coupled across different regions of the atmosphere, we can discern and understand the GW evolution and accurately interpret the data. GWs observations are, however, susceptible to significant line-of-sight (LOS) effects when imaged through deep layers of the atmosphere. These are often not sufficiently characterized in analyses and can have a significant impact on the calculated wave parameters. At large viewing angles intensity enhancements due to LOS effects can improve the observability of waves with large horizontal wavefronts, or, on the other hand, overestimate the amplitude of vertical waves at high altitudes at near-zenith. We investigate realistic LOS effects and observables by using a framework that simulates imaging instruments; integration through volumes of simulation data represents the imaging operation while the instrument's viewing geometry (e.g. camera transformation) is calculated using ray-tracing. We employ the outputs of the compressible atmospheric dynamics model "MAGIC" and the self-consistent multi-fluid ionosphere model "GEMINI" [Zettergren and Snively, JGR, 120, 2015]. Simulations are constructed with physically-constrained convective sources of GWs at midlatitude. Outputs include species and electron densities, and emission rates for multiple airglow layers (OH, oxygen); these allow us to simulate observable data as measured by different imaging instruments: stratospheric CO2 radiance (~35 km peak), as measured by the AIRS IR spectrometer onboard the Aqua satellite [Aumann et al., IEEE, 41, 2003]; mesospheric OH(3,1) band emissions (~87 km peak), observed from ground or space and the OI 630 nm (~250 km peak) emission, observed by ground-based all-sky imagers such as MANGO [Bhatt and Kendall, AGU FM, 2017]. Simultaneously, we model TEC maps (with IPP heights ~300 km), as measured by GNSS receivers. Using these "observables", we investigate and characterize LOS effects through multiple layers that are frequently measured in experiments, and demonstrate constraints placed on real observations from ground or space, towards enabling rigorous model-data comparisons.

MLTG04 - Investigation of a gravity wave ducting event in the upper mesosphere - by Anthony Caton

Status of First Author: Student IN poster competition Masters

Authors: Anthony Caton, Fabio Vargas, Gary Swenson

Abstract: Atmospheric gravity waves (GWs) play an important role in the transport of energy and momentum throughout the Earth's atmosphere. The physical processes associated with GWs must be understood in order to better parameterize their effects on the atmosphere in global climate models. Ducting is a process that can occur when a GW becomes trapped between two evanescent regions in the atmosphere. According to the linear GW theory, a fully ducted wave has zero vertical momentum flux, so the ducting process must also be understood in order to improve our parameterization of GWs in global climate models. In this work, correlative lidar and airglow observations of a highly resonant ducting event, which occurred on the night of January 18, 2015, above the Andes Lidar Observatory (ALO) on Cerro Pachón, Chile (30.0° S, 70.0° W), are presented and analyzed. A ducted quasi-monochromatic GW with large associated temperature (T') and vertical wind (w') perturbations and a period of about 40 min was observed in the mesopause region. A coherent phase relationship, consistent with the linear GW theory, between the temperature and vertical wind perturbations associated with the GW was found. The results also appear to show the generation of a secondary upward-propagating wave above the primary duct.

MLTG05 - Seasonal characteristics of mesospheric short period gravity waves observed on all-sky camera at King Sejong Station (62°S, 59°E) - by Hosik Kam

Status of First Author: Student IN poster competition Masters

Authors: Hosik Kam, Yong Ha Kim, Jeong-Han Kim, Takuji Nakamura, Masaki Tsutsumi, Yoshihiro Tomikawa, Masaru Kogure, Septi Perwitasari

Abstract: We analyzed mesospheric gravity waves in OH airglow images observed during 2012- 2016 by an all-sky camera at King Sejong Station (KSS; 62°S, 58°W), Antarctica. Using a new method of 2D image analysis recently developed by Matsuda et al. (2014), we obtained power spectra of horizontal phase velocity from the image sequence of total 107 image windows. We found from total power spectrum density that wave activity is maximized during winter, as is previously known. We also derived wind blocking fields from MERRA2 reanalysis data for the altitudes 10 - 64 km and from KSS meteor radar data for 80 - 90 km. By comparing the dominant propagating direction of short period gravity waves with the wind blocking field, we found a significant anti-correlation between wind blocking fields and dominant propagating direction of gravity waves except fall season, indicating wind filtering effects. The finding is the direct evidence of wind filtering effects observed in the mesosphere. During fall, the wind blocking fields below ~40 km are not matched with the dominant propagating directions. Thus, we suggest that mesospheric gravity waves observed by the all-sky camera during fall were generated above ~40 km (upper stratosphere and lower mesosphere), probably due to secondary waves. This exception will open up theoretical questions in middle atmosphere dynamic research area.

MLTG06 - AN EXAMINATION OF ATMOSPHERIC TURBULENCE IN THE 100-105 KM REGION OVER CERRO PACHÓN, CHILE - by Channing Philbrick

Status of First Author: Student IN poster competition Masters

Authors: Channing P. Philbrick, Gary R. Swenson. Fabio A. Vargas, Alan Z. Liu

Abstract: Turbulence activity is measured between 100-105 km altitude using a sodium (Na) resonance-fluorescence lidar system for the first time. Previous approaches have been limited to altitudes below 100 km due to sparse Na layer density above 97 km. Using the lidar system at the Andes Lidar Observatory in Cerro Pachón, Chile (30.3°S, 70.7°W), a novel reconstruction algorithm measuring turbulence fluctuation power at smaller signal-to-noise ratios (SNRs) than existing methods is derived and validated. Results are compared against instability, Na mixing ratio, and total constituent diffusion coefficient measurements. Twenty-seven nights of lidar data spanning 2500 hours in the zenith and 2375 hours in the off-zenith directions at 25-m, 6-s resolution were analyzed to determine mean turbulence and instability trends in the mesosphere and lower thermosphere (MLT) region. It was found that average turbulence activity increases in a log-scale linear fashion between 93-100 km altitude, maximizing at 100 km. Above 100 km, turbulence power decays to a local minimum at 102.5 km. Richardson number and Na mixing ratio profiles can successfully identify regions of increased turbulence activity in the 85-105 km region, but fail to determine the relative turbulence power of the regions. Measurements of turbulence activity in the 100-105 km region improve understanding and modeling of atmospheric variability.

MLTG07 - Investigating Short-Term Variability of Mesospheric Gravity Waves Over Antarctica Kenneth Zia and the Atmospheric Imaging Lab - by Kenneth Zia

Status of First Author: Student IN poster competition Masters

Authors: Kenneth Zia, Mike Taylor, Dominique Pautet, Yucheng Zhao, Takuji Nakamura, and Masaru Kogure

Abstract: Short-period (<1 hr) atmospheric gravity waves (GWs) are known to contribute a large potion of the energy and momentum flux into the upper Mesosphere Lower Thermosphere (MLT region ~80-100 km). Knowledge of the parameters of these waves' (i.e. amplitude, phase velocity, wavelength, and period) is essential for understanding the dominant sources of GWs and their impact within the upper atmosphere. The ANtactic Gravity Wave Instrument Network (ANGWIN) is an international collaboration geared to studying the propagation of gravity waves over the Antarctic continent. The Utah State University (USU) Atmospheric Imaging Lab (AIL) operates five all-ski airglow imagers (ASI) and two Advanced Mesospheric Temperature Mappers (AMTMs) at several international sites around Antarctica as well as at South Pole station which investigate GWs in the OH layer (~87 km). A large amount of image data obtained over the past seven years is requiring greater automation in the analysis of the wave parameters. Japan's National Institute of Polar Research's (NIPR's) Space and Upper Atmospheric Physics Group have developed a 3D-FFT method to analyze ASI data [Matsuda et al. 2014] enabling a significant improvement over the individual GW event analysis. They have shared their software capability with USU as part of the ANGWIN collaboration. This poster demonstrates this new quasi-automatic analysis technique applied to high-resolution AMTM intensity and temperature data from McMurdo station (78° S), focusing on a new capability to quantify the GW parameters over hourly time scales and to determine wave characteristics' variability during the Antarctic night.

MLTG08 - Seasonal Trends of Persistent Gravity Waves in Mesosphere and Lower Thermosphere above McMurdo, Antarctica - by Zhuoying Chen

Status of First Author: Student IN poster competition Undergraduate

Authors: Zhuoying Chen, Ian Geraghty, Zimu Li, and Xinzhao Chu

Abstract: Gravity waves play an important role in the upper atmosphere environment. It may even affect global climate change and possibly influence the satellite drag. An Fe Boltzmann lidar installed at McMurdo (77.84 °S, 166.67 °E), Antarctica has been observing gravity wave signatures since Dec 2010. Chen et al. [2016] described the discovery of persistent gravity waves in the MLT region and characterize their properties in the month of June. Following this discovery, Zhao et al. [2017] and Chu et al. [2018] traced the waves to the stratosphere and analyzed the wave features and potential energy density from 30 to 50 km over the five years from 2011 through 2015. In addition, Lu et al. [2015] analyzed three years of winter month data and showed the potential energy density varying considerably from the stratosphere to the MLT. Now we have more than eight years of lidar data from McMurdo and our major goal in this study is to characterize the potential energy density through the whole year. A major issue is how to remove the noise-induced variance from the total variance, and we will try the spectral proportion method. To address the issue of low signal to noise ratio in summer, we will utilize both Fe temperature and Fe density data. We hope to quantify the differences between summer and winter in gravity wave activity at Antarctica.

MLTL01 - Relationship between turbulence and atmospheric stabilities - by Fan Yang

Status of First Author: Student IN poster competition PhD

Authors: Fan Yang, Alan Liu

Abstract: We report a detailed analysis of the stability parameters based on high-resolution temperature and horizontal wind measurements obtained with a Na Lidar at Andes Lidar Observatory (ALO, 30.2°S,70.7°W) and at Maui, HI, USA (20.7°N, 156.2°W). We also demonstrate that the lidar at ALO is capable of detecting the transport effects of turbulence. Combining these two results, we examine the seasonal variations of the stability properties and their relationship with key turbulence parameters including the energy dissipation rate and the turbulence heat transport.

MLTL02 - Probing the analytic CF relationship using Mesospheric Nightglows and Lidar observations obtained at ALO - by Javier Fuentes

Status of First Author: Student IN poster competition Masters

Authors: Javier Fuentes, Fabio Vargas

Abstract: We present the first study to test the theoretical relationship of the Cancellation Factor (CF) using T/W Na Lidar data and zenith night airglow observations of the OH and $O(^{1}S)$ emissions. The dataset analyzed was obtained during the observing campaigns in 2015, 2016, and 2017 at the Andes Lidar Observatory (ALO) in Chile. We have used two empirical methods to fit the analytical function described in Vargas et al. (2007) upon the assumption of having saturated waves (damping factor, \beta = 1), vertically propagating waves, and windless atmosphere. We report that the analytic relationship

underestimates the observational model by a factor of ~3 for OH band emission and by ~1.5 for O(^1S) emission line from method 1 and 2. The disagreement might mainly come from the fact that dissipative and freely propagating waves co-exist with saturated waves, and we have not separated waves by their kind in this study. Another possible source of inaccuracy could be introduced by the photochemical scheme used to model the Cancellation Factor. After correcting both models using the weighted mean to account for their uncertainties in each measurement, see Vargas (2018)\cite {vargas18}, we obtained a good agreement respect to the theoretical value, CF = 5.078, for O(^1S) emission line from method 1. In contrast, the observational model deviate by a factor of sim2 from the theoretical value, CF = 3.80, for the OH emission band in both methods. These important measurements provide a useful information to illustrate the fundamental mechanisms of the variation of the phase and amplitude of the airglow in response to Atmospheric Gravity Waves (AGWs) for both layers through the MLT region.

MLTS01 - Comparative study on mesospheric winds measured by Fabry-Perot interferometer and meteor radar at King Sejong Station, Antarctica - by Changsup Lee

Status of First Author: Student NOT in poster competition PhD

Authors: Changsup Lee, Geonhwa Jee, Jeong-Han Kim, and Yong Ha Kim

Abstract: Neutral winds in the mesosphere and lower thermosphere (MLT) have been simultaneously observed by Fabry-Perot interferometer (FPI) and meteor radar (MR) at King Sejong Station (KSS), Antarctica from 2017. The simultaneous optical and radar observations for the neutral atmosphere in the MLT region provide us with an excellent opportunity of discussing inherent discrepancies between two wind measurement techniques based on temporal and spatial range of sampling area. From the composite wind over the observational period, tidal variabilities are successfully captured by both instruments . Although mean winds measured by FPI and MR are found to have no statistically significant differences, the correlation coefficients stay lower than 0.7. This indicates that the FPI observation is probably severely affected by small-scale wind fluctuation from the turbulence and gravity waves while MR can not resolve those phenomena.

MLTS02 - Investigation of the Role of Water Vapor and Temperature in Noctilucent Cloud Formation - by Jennifer Alspach

Status of First Author: Student IN poster competition Masters

Authors: Jennifer H. Alspach, Jintai Li, Richard L. Collins, Katrina Bossert, Bifford P. Williams

Abstract: The Rayleigh Lidar and the Sodium Resonance Wind Temperature Lidar (SRWTL) systems were used to conduct observations during noctilucent cloud (NLC) season in 2018 at Poker Flat Research Range, Chatanika, Alaska (65°N, 147° W). Clear skies occurred and enabled observations during two nights of the 2018 season on July 31-August 1 and August 10-11. Usually the mesosphere warms as August progresses, making NLC formation more likely at the end of July and beginning of August than later in the month. However, NLCs were detected in the lidar data only on the night of August 10-11. No NLCs were detected on the night of July 31- August 1. Microwave Limb Sounder (MLS) data from the Aura satellite is used to characterize the mesosphere over Alaska during the 2018 NLC season. MLS temperature and water vapor anomalies are examined to determine the relative importance of temperature and water vapor in the

formation of NLCs. This work addresses the recent study by Lübken and colleagues which suggests that increased water vapor in the mesosphere has been the primary driver for NLC enhancement in the past decades [Lübken et al 2018].

MLTS03 - Evaluation of estimated mesospheric temperatures from 11-year meteor radar datasets of King Sejong Station (62S, 59E) and Esrange (68N, 21E) - by Jeong Han Kim

Status of First Author: Non-student PhD

Authors: Jeong-Han Kim, Hosik Kam, Yong Ha Kim, Nicholas Mitchell, Changsup Lee

Abstract: We have evaluated the reliability of two methods for estimating mesospheric temperatures from all-sky VHF meteor radar data. The first method utilizes the decay time of meteor trails, and the other method takes advantage of the linear relation between temperatures and the full width at half maximum (FWHM) of the observed meteor echoes height distribution. We estimated the temperatures from two meteor radar datasets of King Sejong Station (62.22° S, 58.78°E), Antarctic and Esrange, Sweden (67.90° N, 21.10°E) during a period of 2007 to 2017 and 2003 to 2013, respectively. We devised an improved decay time method of temperature estimation that utilizes careful selection of detected echoes by reflecting seasonal change in height range where ambipolar diffusion is dominant in meteor decay. Applying the improved method, we achieved temperature estimation on average within 4.9 and 5.4% from Aura/MLS temperatures at 90 km at Esrange and KSS, respectively. In comparison, temperatures estimated by the FWHM method have averaged differences of 5.3 and 3.6% from the MLS temperatures at Esrange and KSS, respectively. However, the FWHM temperatures show significantly less temporal fluctuations than the temperatures estimated by the decay time for both sites. This may indicate that the FWHM method is more robust to estimate mesospheric temperatures from meteor radar data.

MLTT01 - Structure and Seasonal Variation of Migrating Tides in the Whole Atmosphere Community Climate Model with Thermosphere and Ionosphere Extension (WACCM-X) - by Yi Chung Chiu

Status of First Author: Student IN poster competition PhD

Authors: Yi Chung CHIU, Cornelius Csar JUDE, Loren CHANG

Abstract: The Whole Atmosphere Community Climate model – eXteended (WACCM-X) is a comprehensive numerical model with a range from the Earth's surface to the upper thermosphere (~ 500 km) and also includes the ionosphere. In this study, we used the least squares method to extract diurnal and semidiurnal migrating tides from free running WACCM-X temperatures in the mesosphere and lower thermosphere region (MLT). The results are compared to tides in Specified Dynamics WACCM (SD-WACCM) and observations from TIMED/SABER. Differences in tidal structure and variation during solar maximum and minimum in March and June are examined, to better understand the fidelity of migrating tides resolved in free running WACCM-X, and its implications for future studies utilizing this model.

MLTT02 - Wavenumber diagnosis of mesospheric global-scale waves using a limited number of specular mentor radars - by Maosheng He

Status of First Author: Non-student PhD

Authors: Maosheng He, Jorge Luis Chau, Guozhu Li, Peter G. Brown, Dmitry V. Korotyshkin, Gunter Stober, and Dmitry Pokhotelov

Abstract: Mesospheric waves are often identified from specular meteor radar (SMR) observations through spectral analysis using single-radar techniques which cannot resolve the wave's spatial scale. Therefore, the resolved spectral signature at a given frequency might comprise contributions from multiple-scale waves. In a series of works, we developed approaches using a limited number of radars to diagnose the wavenumber associated with spectral signatures seen in individual radar observations. The approaches joint several analysis methods, including Fourier transform, wavelet analysis, cross-wavelet analysis, phase differencing analysis, and least square regression analysis. We implemented the approaches to a couple of dual- and tri-radar configuations at latitudes between 45°N and 70°N. By constraining both frequency and wavenumber, our implements identified various waves, including migrating solar and lunar tides at the period of 12.4h. 12h, 8h, 6h, 4.8h, 4h, non-migrating solar tides at 12h period, 10- and 16-day planetary normal modes, secondary waves of nonlinear interactions between migrating tide and planetary waves. Specifically, both case and statistical studies suggest that most of the identified waves respond significantly to sudden stratospheric warming events (SSWs): most migrating solar tides and the planetary waves weaken whereas the lunar tide and secondary waves enhance. Our results also suggest the enhancement of two secondary waves of nonlinear interaction between the 16-day wave and 12h migrating tide during SSW have been misinterpreted as two non-migrating solar tides.

MLTT03 - Observations of the Semidiurnal Tide in ALO-USU Rayleigh Lidar Mesospheric Temperature Observations - by jonathan price

Status of First Author: Student IN poster competition PhD

Authors: Jonathan Price, Vincent Wickwar

Abstract: Solar atmospheric tides are global-scale oscillations observable in such parameters as temperature, density and wind. They primarily originate in the troposphere and stratosphere through UV and IR solar radiation absorption and propagate upwards transporting energy and momentum into the middle and upper atmosphere. Mesospheric temperatures obtained during 11 years of observations with the ALO-USU, Rayleigh-scatter lidar system are used to investigate mesospheric semidiurnal tidal amplitudes and phases. Hourly temperature profiles are derived throughout each night. These profiles are then averaged over multiple nights. At each altitude between 45 and just above 85 km, an average temperature is found using a 31-night running window centering on a given night and including 15 nights on either side of it. These resultant hourly profiles are fitted at each altitude using a 12-hour cosine function to extract the nightly semidiurnal tidal amplitudes and phases. In addition, these nightly amplitudes and phases from the profiles are averaged over the eleven years of data to obtain a composite climatology of the semidiurnal amplitudes and phases, and to obtain interannual variability in these parameters. Furthermore, differences between the annual and composite year climatologies provide insights into the year-to-year variability.

MLTT04 - Latitudinal difference in responses of the MLT region to the sudden stratospheric warming events - by Yuyan Jin

Status of First Author: Student IN poster competition Masters

Authors: Yuyan Jin, You Yu

Abstract: Sudden Stratospheric Warming (SSW) is a common phenomenon in the polar winter stratosphere. It shows a sudden rise in temperature followed by a decrease or even reversal of eastward winds, due to the interaction of waves and background flow. In the present work, we examine the response of the MLT region in the middle and low latitudes to the 2017 SSW using the wind observations from a four-station meteor radar chain along the 120°E meridian. The measured winds are considered to be a superposition of mean wind and different oscillations including diurnal tide, semidiurnal tide and quasi 2-day waves (QTDWs). We fit zonal and meridional components independently in a 6-day window shifted by 1-day to get the amplitudes of every oscillation. The results show that the amplitudes of the diurnal tide and QTDWs in the observation region enhanced during SSW events. Stronger enhancement appeared in low (middle) latitude for the meridional (zonal) oscillations of diurnal tide and QTDWs. It's noteworthy that a polar event has a more significant impact on low latitude instead of higher latitude region for the meridional oscillations. Unlike the results reported before, there is no obvious enhancement for the semidiurnal tide in our observation. Furthermore, we examine two more SSW events during winter of 2013-2014, 2017-2018 and get the similar findings.

MLTT05 - Statistics on nonmigrating diurnal tide generated by tide-planetary wave interaction and their relationship to Sudden Stratospheric Warming - by Jian Du

Status of First Author: Non-student PhD

Authors: Xiaojuan Niu, Jian Du, Xuwen Zhu

Abstract: The nonmigrating diurnal tide, DW2, is known to have a source from the stationary planetary wave with wavenumber 1 (SPW1) and the migrating diurnal tide (DW1) interaction. Recent research has shown that DW2 time evolution in the equatorial mesopause tracks very well with SPW1 in the polar stratosphere for the winter of 2009–2010, which contains a sudden stratospheric warming (SSW) vortex split event. This paper extends previous research and investigates the relationship between these two waves for 31 winters from 1979 to 2010 with the extended Canadian Middle Atmosphere Model (eCMAM) through correlation and composite analysis. Significant correlations are present between the two waves in 20 out of 31 winters (65%). We separate the 31 winters into four categories: SSW-displacement, SSW-split, minor-SSW, and no-SSW. Our results show that there is no significant difference among the four categories in terms of correlations between the two waves. Although SPW1 is usually stronger during a SSW-D winter, this does not warrant a stronger interaction with DW2.

MLTT06 - Statistical Modeling of Tidal Weather in the Mesosphere and Lower Thermosphere - by Jian Du

Status of First Author: Non-student PhD

Authors: Jian Du, Ashan Vitharana, Xuwen Zhu, Jens Oberheide, William E. Ward

Abstract: We study the statistical properties of tidal weather (period < 30 days) of DW1 amplitude using the extended Canadian Middle Atmospheric Model (eCMAM) and Sounding of the Atmosphere using Broadband Emission Radiometry (SABER). A hierarchy of statistical models, e.g. the auto-regressive (AR), vector AR (VAR), and parsimonious vector AR (PVAR) models, are built to predict tidal weather. The quasi 23-day oscillation found in the tidal weather is a key parameter in the statistical models. Comparing to the more complex VAR and PVAR models, which consider the spatial correlations of tidal weather, the simplest AR model can predict day-1 tidal weather with an accuracy of 89%. In the AR model, 23 coefficients at each latitude and height are obtained from 7 years of eCMAM data. Tidal weather is predicted via a linear combination of 23-day of tidal weather data prior to the prediction day. Different sensitivity tests are performed to prove the robustness of these coefficients. These coefficients obtained from eCMAM are in very good agreement with those from SABER. The SABER tidal weather is predicted by AR model with coefficients from eCMAM and SABER with an accuracy of 86% and 87% at day-1, respectively.

MLTT07 - Nonmigrating Tidal Variability on Planetary Wave-scales in the Mesosphere and Lower Thermosphere Region from SABER - by Komal Kumari

Status of First Author: Student IN poster competition Masters

Authors: Komal Kumari, Jens Oberheide

Abstract: The prominent eastward-propagating nonmigrating diurnal tide with zonal wave number 3 (DE3) can reach into the mesosphere and the upper thermosphere (80-100 km), introducing longitudinal and large day-to-day variability in temperature, wind and density. In this article, we discuss the physical reasons for the observed tidal variability on planetary wave timescales from 16 years of SABER (onboard TIMED satellite) tidal deconvolution diagnostics. The methodology uses an Information-theoretic approach based on Bayesian statistics, time dependent probability density functions and Kullback-Leibler divergence. We will also discuss the interannual and intra-annual statistical characteristics of the short-term DE3 variability associated with the quasi-biennial oscillation (QBO), El Niño-Southern Oscillation (ENSO), solar cycle and other natural drivers.

MLTT08 - Statistical Modeling of DE3 Tidal Variability in the MLT Region - by Ashan Vitharana

Status of First Author: Student IN poster competition Masters

Authors: Ashan Vitharana1, Jian Du1, Xuwen Zhu2, Jens Oberheide3, William E. Ward

Abstract: In this research we attempt to build a model to predict day to day tidal variability of the DE3 using an empirical statistical model based on auto regression (AR). We will present some of the statistical properties of the day-to-day variability of the tide, and the process to build the model to understand and simulate the complex tidal variability from a statistical point of view using Sounding of the Atmosphere using Broadband Emission Radiometry (SABER) temperature observations in the Mesosphere and lower Thermosphere (MLT) region and extended Canadian Middle Atmospheric Model (eCMAM) data.

MLTT09 - Modeling Study of Short-term Variability of Migrating Diurnal Tide - by Jack Wang

Status of First Author: Student IN poster competition PhD

Authors: Scott Palo, Hanli Liu

Abstract: Migrating diurnal tide (DW1) is known to be one of the dominant factors in governing the dynamics of the mesosphere and lower thermosphere (MLT). It is variable at different time scales, from days to years. The causes of the long-term variability are well characterized through decades-long investigating by the community. On the other hand, the driving mechanisms for short-term variability, which is important for studying the weather of the thermosphere and ionosphere, are still not well understood. This research aims to determine potential causes driving the short-term variability of DW1, including wave source, mean state, and the gravity wave. The variability of the wave source and the mean state will be determined by analyzing the output of the NCAR Whole Atmosphere Community Climate Model with thermosphere/ionosphere extension (WACCM-X). The WACCM-X output will then be used to constrain the background state of the Thermosphere Ionosphere Mesosphere Electrodynamics General Circulation Model (TIME-GCM) simulation, with wave sources specified either by the climatological GSWM or the variable WACCM-X output at the lower boundary. We can determine the contribution of each potential driving term to the DW1 variability using these numerical experiments. We found that the day-to-day variability of the mean state plays a major role in driving the DW1 short-term variability. The daily change of DW1 amplitude can be up to 50% in the simulation, and the horizontal structure of DW1 is also sensitive to the mean state. The wave source variability plays a secondary role in driving DW1 variability, which is consistent with previous studies. It can cause ~ 15 to 30 % variation to the DW1 amplitude. On the other hand, the gravity wave modulation to DW1 is relatively small, suggesting its effect might be indirect by modulating the mean state.

PLAN01 - Terminator Structures in the Thermosphere and Ionosphere of Mars - by Marcin Pilinski

Status of First Author: Non-student PhD

Authors: Steve Bougher, Laila Andersson

Abstract: The NASA Mars Atmosphere and Volatiles EvolutioN (MAVEN) spacecraft has been collecting data in the Martian atmosphere since November 2014. MAVEN observations of the Martian thermosphere have indicated the presence of persistent density and temperature structures near the dawn and dusk terminators. The persistence of these features is inferred from the fact that they are observed in similar locations over the course of different seasons and years. These features were first termed "heat islands" by Bougher et al. (1990) who predicted their existence in early models of the Martian thermosphere. We explore the MAVEN neutral composition and ionospheric density data using in-situ measurements and identify near-dusk neutral temperature and density enhancements. This analysis spans repeated visits of the dusk terminator by the MAVEN orbit periapsis. We compare the data with global circulation model results generated for solar conditions corresponding to the time of measurement. The model and data indicate a large-scale temperature perturbation between 18-20 LST.

PLAN02 - Variability and Phenomenology of Proton Aurorae at Mars as Observed by MAVEN/IUVS - by Andrea Hughes

Status of First Author: Student IN poster competition PhD

Authors: Andréa Hughes, Michael Chaffin, Edwin Mierkiewicz, Justin Deighan, Sonal Jain, Nicholas Schneider, Majd Mayyasi, Bruce Jakosky

Abstract: We present observations of proton aurora at Mars using the Imaging UltraViolet Spectrograph (IUVS) onboard the Mars Atmosphere and Volatile EvolutioN (MAVEN) spacecraft. Proton aurora are a third type of aurora identified at Mars in addition to discrete and diffuse aurora (Deighan et al., 2018). Terrestrial proton aurora are strongly influenced by Earth's global magnetic field. Alternatively, due to Mars' lack of a planetary-wide magnetic field, Martian proton aurora are constrained to the dayside and form via electron stripping and charge exchange with the neutral corona. We present a comprehensive database of events characterizing the proton aurora dataset and describing their variability. We use altitude-intensity profiles of hydrogen Lyman-alpha (121.6 nm) IUVS periapsis limb scan data. Martian proton aurora profiles display a prominent peak in this emission between ~110-150 km altitude. We observe this characteristic proton aurora signature in ~14% of dayside periapsis profiles from the entire mission (~2 Martian years). These detections make proton aurora the most common type of aurora currently observed at Mars. Further, we observe that proton aurora have low solar zenith angles (SZA) and occur primarily on the Mars dayside, consistent with known formation mechanisms. We also observe that proton aurora have highest emission enhancements, peak intensities, peak altitudes, and occurrence rates around southern summer solstice. This time period corresponds to when the neutral atmosphere is inflated, hydrogen coronal densities are increased, and the Mars-Sun distance is small following perihelion. We determine that the primary factors influencing proton aurora magnitude and occurrence are season and SZA. These results provide a deeper understanding of the phenomenology of proton aurora as observed over multiple Mars years, as well as primary influences on and annual variations in these events. By studying proton aurora at Mars we may better understand the connection between the solar wind and Mars' hydrogen corona, which in turn informs our understanding of other planetary bodies that exhibit a neutral hydrogen corona and lack a global magnetic field.

PLAN03 - Tidal waves observed in both the ionosphere and thermosphere: Results from in-situ measurements at Mars - by Scott Thaller

Status of First Author: Non-student PhD

Authors: Scott Thaller, Laila Andersson, Marcin Pilinski

Abstract: Through the collisional coupling between the ionosphere and thermosphere, dynamic processes in the thermosphere with timescales longer than the equilibrium timescale will drive corresponding processes in the ionosphere. The thermosphere of Mars contains tidal waves in which the fluctuations are on the order of 20% of the ambient thermosphere density. Below ~200 km the ions are demagnetized and the ionosphere can respond to large (~20%) changes in the thermosphere on timescales of less than 1 hour. As a result, the ionosphere moves with the tidal motion of the thermosphere. In this poster, we present initial work on examining these tidal wave perturbations in the ionosphere and thermosphere of Mars. The ionospheric electron density measurements in this study are made with the Langmuir Probe and Waves (LPW) instrument, and thermosphere densities are measured by the Neutral Gas and Ion Mass Spectrometer (NGIMS), both on the MAVEN satellite. MAVEN has an orbit with periapsis extending below ~150 km. For context, this altitude on Mars is the equivalent of Earth's E-region. We further use the Mars Climate Database (MCD) which is a database of meteorological fields derived from General Circulation Model numerical simulations of the Martian atmosphere and validated against observational data. We observe mode 3 waves (event analyzed happens to be on the day side) in which the density variations are mainly positively correlated and, in a separate case on the night side, we observe mode 3 waves in the ionosphere at high altitude while possibly mode 2 < ~170 km, out of phase with model mode 2 waves. Time periods where the observed electron and neutral densities and model densities all have the same wave-mode and phase are clearly seen. Because the MAVEN satellite makes in-situ measurements in the equivalent of Earth's E-region and above, at Mars we can study the breaking and vertical propagation of these large scale waves.

SOLA01 - Empirically Guided Modeling of the Ionosphere With Ionosonde Measurment Comparisons of the 2017 Solar Eclipse - by Lee Kordella

Status of First Author: Student NOT in poster competition PhD

Authors: Lee J. Kordella, Gregory D. Earle, Douglas P. Drob, Joseph D. Huba

Abstract: Rigorous modeling efforts have been carried out to accurately recreate the spatio-temporal variation of the solar EUV flux due to the 2017 Great American Solar eclipse. In order to better understand the eclipse effects we have integrated empirical observations of the solar disc on the eclipse day in conjunction with sun, moon earth position calculations into the SAMI-3 global ionospheric model. Here we compare the model results with those of vertical incidence HF ionospheric sounder data collected by Virginia Tech. A discussion of key features observed on the event day including the presence of sporadic E and the ionspheric G condition follows.

SOLA02 - Using Orbit Propagation to Probe the Thermospheric Dynamic Response to Geomagnetic Energy Input - by Daniel Brandt

Status of First Author: Student IN poster competition Masters

Authors: Brandt, Daniel A., Bussy-Virat, Charles D., and Ridley, Aaron J.

Abstract: The thermosphere is the home of the International Space Station, numerous research satellites, and a plethora of space debris. It is the region of the atmosphere for which nearly all Extreme Ultraviolet radiation is absorbed. The neutral density of the thermosphere is highly responsive to diurnal variation, changes in EUV radiation, and fluctuations in the interplanetary magnetic field. Empirical atmospheric models, the most accurate of which is NRLMSISE-00, poorly model the thermospheric density response during geomagnetic storms, reducing the accuracy of orbital propagators, hampering our ability to estimate the time and location of satellite reentry, and jeopardizing our ability to perform accurate spacecraft collision avoidance. Most significantly, they reflect a major gap in our understanding of the nature and effects of magnetospheric energy input into the thermosphere. We demonstrate an observable bias in density under-prediction during geomagnetic storms by NRLMSISE-00 in the lower thermosphere using CubeSat two-line element sets (TLEs), and propose a method for investigating and rectifying the observed inaccuracy using TLEs and an in-house orbital propagator, the Spacecraft Orbital Characterization Kit (SpOCK), to develop a calibration algorithm that results in the maximum of orbit error. This method will not only serve to improve our capabilities of space situational awareness, serving the needs of science, industry, and military alike, but will enable us to gather more insight into the nature of the thermospheric reaction to enhanced geomagnetic and solar activity.

SOLA03 - Simulating Global-scale Observation of Limb and Disk's (GOLD) measurement of the July 2nd, 2019 total solar eclipse's effect on the Ionosphere-Thermosphere system. - by Saurav Aryal

Status of First Author: Non-student PhD

Authors: Saurav Aryal, Tong Dang, Huixin Liu, Geonhwa Jee, Jiuhou Lei, Wenbin Wang, Alan G Burns, Stanley C Solomon and Richard Eastes

Abstract: A total solar eclipse will occur in the southern hemisphere on July 2, 2019 from approximately 17 to 22 UT. It will cross South America where it's effects can be observed from a geostationary orbit by the Global-scale Observation of Limb and Disk (GOLD) instrument. GOLD will observe the changes in OI 135.6 nm and N2 LBH band emissions, which will be used to derive changes in composition ratios, neutral temperatures on the dayside and peak electron densities on the nightside as a result of the eclipse. Simulations of the eclipse's effects on the Ionosphere-Thermosphere (I-T) system, as seen by the GOLD instrument, have been performed using the Thermospheric General Circulation Model (TGCM) and the GLobal airglOW (GLOW) model. Calculation show small but observable differences in the daytime airglow brightnesses and temperatures. The results obtained are being used to deduce the required measurement criteria for GOLD to successfully observe the expected changes. The magnitudes and temporal-spatial development of these changes can be compared with observations. This comparison will provide a test for our understanding of the eclipse's effects on the I-T and their origin.

SOLA04 - Analysis of the August 2017 Eclipse's Effect on Radio Wave Propagation Employing a Raytrace Algorithm - by Magdalina Moses

Status of First Author: Student IN poster competition Masters

Authors: Magdalina Moses, Lee J. Kordella, Gregory D. Earle, Douglas Drob, Joseph D. Huba, Shantanab Debchoudhury

Abstract: The total solar eclipse over the continental United States on August 21, 2017 offered a unique opportunity to study the dependence of the ionospheric density and morphology on incident solar radiation. Unique responses may be witnessed during eclipses, including changes in radio frequency (RF) propagation at high frequency (HF). Such changes in RF propagation were observed by the Super Dual Auroral Radar Network (SuperDARN) radars in Christmas Valley, Oregon and in Fort Hayes, Kansas during the past summer's eclipse. At each site, the westward looking radar observed an increase in slant range of the backscattered signal during the eclipse onset followed by a decrease after totality. In order to investigate the underlying processes governing the ionospheric response to the eclipse, we employ the HF propagation toolbox (PHaRLAP), created by Dr. Manuel Cervera, to simulate SuperDARN data for different models of the eclipsed ionosphere. By invoking different hypotheses and comparing simulated results to SuperDARN measurements we can study the underlying processes governing the ionosphere and improve our model of the F-Region responses to an eclipse.

SOLA05 - The Role of the Solar Soft X-ray Irradiance on Thermospheric Chemistry and Structure - by Srimoyee Samaddar

Status of First Author: Student NOT in poster competition PhD

Authors: Srimoyee Samaddar, Karthik Venkataramani, Scott Bailey

Abstract: The solar soft x-ray irradiance deposits energy into the lower thermosphere, thus playing a significant role in the photochemistry and E-region ionosphere. Since the irradiance varies strongly with solar activity, it is imperative to incorporate this variability in models predicting the earth's thermosphere. In this talk, we use the recently developed ACE1D model to explore the role of solar soft x-rays on temperature, chemistry, and the overall structure of the thermosphere. The ACE1D model produces a global average thermosphere by self- consistently solving the one-dimensional continuity equations to obtain the ions and neutral densities and the energy equations to obtain the ions, neutral and electron temperatures. A combination of solar and magnetospheric fluxes and joule heating is used as energy inputs to the model. We show that solar soft X-rays are the dominant driver of globally averaged nitric oxide densities. We further find that the soft x-rays have a very large impact on temperature throughout the thermosphere, even though their energy is deposited low in the thermosphere. We show that this is due to the heat exchange from non-thermal electrons which plays a significant part in energy dynamics of the thermosphere.

SOLA06 - Geocoronal Hydrogen Emission Variation Over Two Solar Cycles - by Susan Nossal

Status of First Author: Non-student PhD

Authors: S. M. Nossal, E.J. Mierkiewicz, F.L. Roesler, R.C. Woodward, D.D. Gardner, L. M. Haffner

Abstract: Ground-based hydrogen Balmer-α observations from Northern mid-latitudes span multiple solar cycles, facilitating investigation of decadal scale variations, including natural variability in the hydrogen response to solar geophysical changes. We will present a reanalysis of ground-based hydrogen emission observations from the early 1990s, based on a detailed review of the calibration procedures, and their comparison with observations obtained in 2000-2001 in the context of the extended Northern hemisphere mid-latitude geocoronal hydrogen emission data set. This work suggests a likely increase in hydrogen emission intensity between the solar-maximum period of 1990-1991 (solar cycle 22) and the near-solar-maximum period of 2000-2001 (solar cycle 23), with the caveat that this is a limited data set and that there are calibration uncertainties. The apparent increase in intensity is counter to previous observations from mid-latitudes in which the observed intensity increases with higher solar activity. Additionally, the apparent increase in intensity is of larger magnitude than model simulations predict the response would be due to increases in greenhouse gases. The detailed review of the calibration procedures has also provided insights to guide design of future observations.

SOLA07 - The role of H geocorona dynamics in storm-time ring current recovery - by Gonzalo Cucho-Padin

Status of First Author: Student NOT in poster competition Masters

Authors: Gonzalo Cucho-Padin, Lara Waldrop

Abstract: During the slow recovery phase of geomagnetic storms, charge-exchange collisions between ring current ions and hydrogen (H) atoms in the outer exosphere serve to dissipate magnetospheric energy through the generation of energetic neutral atoms (ENAs), which can escape Earth's gravity on ballistic trajectories. Imaging of the resulting ENA flux together with inversion techniques enables the estimation of ring current ion distribution; however, its accuracy depends on the specification of the exospheric H density distribution. Although UV measurements of scattered emission by H-atoms exhibit variations during storm-time, the H density distribution used in ENA image inversion are typically assumed to be temporally static. Hence, the absence of H models that account for its temporal evolution represents a source of significant uncertainty in the estimation of ring current dynamics. Our recent development of a robust tomographic technique for estimation of 3-D global exospheric H density distribution from its UV emission data and the addition of the temporal domain via Kalman filtering overcomes the limitations of the past analyses. In this work, we present the reconstruction of the global, 3D, and time-dependent H density distribution from observations of its optically thin emission at 121.6 nm (Lyman-α) acquired from the Lyman-alpha detectors (LADs) onboard the NASA's Two Wide-angle Imaging Neutral-atom Spectrometers (TWINS) satellites. We use the Hot Electron and Ion Drift Integrator (HEIDI) kinetic model to perform simulations of the ring current and investigate the charge exchange interactions between the resulting H density distribution and ring current ions. We use these simulations to generate synthetic images of ENA flux for comparison with those measured by TWINS ENA imagers, and we also invert actual TWINS ENA images using the time-dependent H density distributions to obtain unprecedented ring current ion sensing that more accurately reflects the dynamic H geocorona.

SPRT01 - Photoionization and electron impact ionization of metallic species at sprite altitudes as a mechanism of initiation of sprite streamers - by Reza Janalizadeh Choobbasti

Status of First Author: Student IN poster competition PhD

Authors: Reza Janalizadeh and Victor P. Pasko

Abstract: As a result of meteoric ablation Fe, Mg, Si, Na, Ca and K atoms form well defined layers in the Earth's atmosphere [Plane et al., Chem. Rev., 115, 4497, 2015], and the overall injection rates of these elements form broad peaks in the altitude range between 70 and 120 km [Plane et al., Space Sci. Rev., 214, 23, 2018]. The local concentration of these elements is expected to depend on meteor mass, velocity, altitude of deposition, and also on the stage of meteor trail expansion. Although these elements initially appear in ionized form, the ions quickly oxidize and then recombine with electrons resulting in the neutral atomic form of these species [Silber et al., MNRAS, 469, 1869, 2017, and references therein] with typical lifetimes measured in hours [Plane et al., Chem. Rev., 115, 4497, 2015]. In terms of relative concentration Fe, Mg, and Si typically dominate, followed by Na, Ca, and K [Plane et al., Space Sci. Rev., 214, 23, 2018; Granier et al., GRL, 16, 243, 1989]. It is remarkable that all these species have ionization thresholds: Fe (7.9 eV, 157 nm), Mg (7.64 eV, 162 nm), Si (8.15 eV, 152 nm), Na (5.13 eV, 242 nm), Ca (6.11 eV, 203 nm) and K (4.34 eV, 286 nm) much below the main constituents of air: N2 (15.60 eV, 80 nm) and O2 (12.06 eV, 102.5 nm), allowing them to be effectively ionized in collisions with relatively low energy electrons. These species can also be photoionized by UV photons associated with various band systems of N2 emitted by sprite halo discharges. We calculate electron impact ionization rates of these metals by inputting published ionization cross section data [e.g., Boivin et al., J. Phys. B: At. Mol. Opt. Phys., 31, 2381, 1998; Kim et al., J. Phys. B: At. Mol. Opt. Phys., 40, 1597, 2007] to BOLSIG+ software [G. J. M. Hagelaar, L. C. Pitchford, PSST, 14, 722, 2005]. For photoionization calculations we assume that UV photons originate from the same singlet states of N2 that lead to classical photoionization of O2 in air [Zheleznyak et al., High Temp., 20, 357, 1982]. In addition, we consider UV emissions from Lyman-Birge-Hopfield (LBH) band system of N2 which has an emission spectrum in the range 120-280 nm [A. V. Vallance Jones, Aurora, 134, 1974] and is abundantly produced in sprites. We note that LBH N2 emissions are only able to photoionize metallic species, while emissions originating from the N2 singlet states are capable of photoionizing both O2 and metallic species. In order to calculate the photoionization rates due to seeds of metallic species, we develop first principles models of radiative transfer of photoionizing photons through the air medium. Finally, we employ a plasma fluid model of sprite halo to compare streamer initiation from a gas mixture including various densities of these metals with previous works which artificially assumed high electron density regions in the simulation domain [e.g., Qin et al., GRL, 40, 4777, 2013; Qin et al., JGR, 118, 2623, 2013].

SPRT02 - Gigantic Jets Observed from Geostationary Orbit - by Levi Boggs

Status of First Author: Student IN poster competition PhD

Authors: Levi D. Boggs, Ningyu Liu, Michael Peterson, Steven Lazarus, Michael Splitt, Frankie Lucena, Amitabh Nag and Hamid K. Rassoul

Abstract: Gigantic jets (GJs) are a type of transient luminous events [Pasko, 2010; Liu et al., 2015a]. They are electrical discharges that exit the tops of thunderstorms and reach 70-90 km altitudes [Pasko et al., 2002; Su et al., 2003], capable of transferring tens to hundreds of coulombs of charge between the thundercloud and the ionosphere [Cummer et al., 2009; Lu et al., 2011; Liu et al., 2015b]. Most observations of gigantic jets come from ground-based low-light-level optical cameras. This observation method is not ideal for monitoring GJ activity, as the camera must have a clear view of the region above thunderclouds. An optimal viewing condition is often unavailable during potential GJ producing storms, because those storm systems (tropical systems at low latitudes) are normally accompanied by substantial areas of stratiform clouds. GJs have also been observed by space-based instruments including the Imager of Sprites and Upper Atmospheric Lightning (ISUAL) onboard the FORMOSAT-2 satellite [Chen et al., 2008]. While ISUAL had dedicated instrumentation to observe GJs, it likely missed a lot of GJ events due to its limited coverage from the low Earth orbit of FORMOSAT-2. However, with the relatively high-resolution imaging capability from the geosynchronous orbit provided by the Geostationary Lightning Mapper (GLM) [Rudlosky et al., 2018], new opportunities are available to detect GJs. GLM is a high-speed (2 ms) optical detector observing emissions in a narrow band at 777.4 nm. The high orbital altitude enables its CCD detector to continuously observe lightning and other terrestrial flashes across nearly an entire hemisphere with a relatively consistent pixel resolution (8 km at nadir and increasing to 14 km at the edge of its field of view) [Goodman et al., 2013]. Here we present the first GLM observations of GJs. The GJs occurred 200-500 km south of Puerto Rico from Tropical Storm Harvey, and were simultaneously recorded by a ground-based low-light-level camera from Puerto Rico. Unlike typical GLM flashes that consist of discrete optical pulses, GJ flashes contain long periods of sustained optical emissions in a fixed, small area in the GLM image. Most of the total optical energy is concentrated in a single GLM pixel in all frames of the GJ, which corresponds to the azimuth of the GJ in the ground-based video recordings.

Rodriguez-Zuluaga, Juan	13
Samaddar, Srimoyee	40
Shidler, Samuel	18
Siddiqui, Tarique Adnan	1
Song, Byeong-Gwon	26
Suclupe Osorio, Jose Manuel	14
Tai, Tzu-Ya	1,2
Thaller, Scott	38
Tyska, Justin	4
Urea, John	25
Vitharana, Ashan	36
Waldron, Zachary	5
Wang, Binghui	20
Wang, Jack	36
Wang, Yu	26
Yang, Fan	30
Zhao, Yuxin	7
Zhou,Xu	23
Zia, Kenneth	29